PURIFICATION AND CHARACTERIZATION OF NAD^+ KINASE FROM RAT LIVER

by

JAMES EDWARD KENNAMER

Bachelor of Science

Oklahoma State University

Stillwater, Oklahoma

1981

Submitted to the Faculty of the Graduate College
of the Oklahoma State University
in partial fulfillment of the requirements
for the Degree of
DOCTOR OF PHILOSOPHY
July, 1986

PURIFICATION AND CHARACTERIZATION

OF NAD+ KINASE FROM RAT LIVER

Thesis Approved:

Robert K. Gholson
Thesis Adviser

Earl D. Mitchell

Charles O. Gardner Jr

Richard C Essenberg

Richard A. Ott

Norman N. Durham
Dean of the Graduate College

ACKNOWLEDGMENTS

The author wishes to thank his major adviser, Dr. Robert K. Gholson, for his encouragement and patience during this work. I also wish to thank Drs. E. D. Mitchell, R. C. Essenberg, C. O. Gardner, and R. A. Ortez for their service as members of my advisory committee and to Drs. G. V. Odell and H. O. Spivey for many helpful discussions. Appreciation is extended to Mrs. Sue Heil for typing this manuscript. The financial support and provision of facilities by the Department of Biochemistry and Oklahoma State University are gratefully acknowledged. I would also like to thank the McAlester Scottish Rite Foundation for their support through a fellowship during this study.

The author is also thankful for the technical assistance of Mr. Paul Swartz and Miss Carol Christian. A special thanks goes to my wife, Susan, for understanding and sacrifice during these studies. Thanks is extended to my parents who have supported and encouraged me throughout my education. I would also like to express my gratitude to Mr. Arthur May for influencing my decision to pursue a scientific career. A very special thanks goes to the students and members of the Department of Biochemistry for making this study an enriching experience.

TABLE OF CONTENTS

LIST OF TABLES

LIST OF FIGURES

LIST OF ABBREVIATIONS

ADP	Adenosine diphosphate
ADPR	Adenosine diphosphate ribose
AMP	Adenosine monophosphate
APAD	3-acetyl pyridine adenine dinucleotide
ATP	Adenosine triphosphate
cAMP	3', 5'- cyclic adenosine monophosphate
CTP	Cytidine triphosphate
dATP	2'- Deoxyadenosine triphosphate
DEAE	Diethylaminoethyl
DHAP	Dihydroxyacetone phosphate
dNAD	Nicotinic acid adenine dinucleotide
DTNB	Dithionitrobenzoic acid
DTT	Dithiothreitol
FAD	Flavin adenine dinucleotide
GTP	Guanosine triphosphate
HMB	Hydroxymercuribenzoate
ITP	Inosine triphosphate
MES	2-[N- Morpholino] ethane sulfonic acid
MOPS	3-[N- Morpholino] propane sulfonic acid
NA	Nicotinic acid
NAD+	Nicotinamide adenine dinucleotide
NAm	Nicotinamide
NaMN	Nicotinic acid mononucleotide
NADP+	Nicotinamide adenine dinucleotide phosphate
NEM	N-ethyl maleimide
NMN	Nicotinamide mononucleotide
OAA	Oxaloacetate
PPi	Inorganic pyrophosphate
PRPP	5-Phosphoribosyl-1-pyrophosphate
QA	Quinolinic acid
TFP	Trifluoperazine
TTP	Thymidine triphosphate

CHAPTER I

INTRODUCTION

The pyridine nucleotides, $NADP^+$ and NAD^+, serve as coenzymes in biological oxidation-reduction reactions. $NADP^+$ is used primarily in pathways of anabolic metabolism, whereas NAD^+ is the coenzyme used in catabolic pathways. Changes in the levels of $NADP^+$ may serve to regulate the flux of metabolites through pathways which use $NADP^+$ as a coenzyme. The key role that $NADP^+$ plays in cellular metabolism has stimulated investigations into its biosynthesis and the regulation of its formation.

$NADP^+$ is formed by the ATP-dependent phosphorylation of NAD^+ catalyzed by NAD^+ kinase. Within plant chloroplasts, NAD^+ kinase requires the presence of Ca^{++} and calmodulin for activity. Calmodulin-dependent NAD^+ kinases have also been identified in several other systems. However, the manner in which NAD^+ kinase is regulated in mammalian tissues remains unclear. This investigation was directed toward elucidating the enzymatic properties of NAD^+ kinase from rat liver. The approach was to purify NAD^+ kinase and explore some of the physical, kinetic, and regulatory characteristics of the enzyme.

CHAPTER II

LITERATURE REVIEW

In 1904, Harden and Young first described the presence of an active component in boiled yeast extracts capable of enhancing fermentation (1). Further studies on this component by Von Euler et al. (2) and Warburg (3, 4) led to the isolation and structural determination of the pyridine nucleotides NAD^+ and $NADP^+$. NAD^+ contains nicotinamide ribose phosphate and adenosine 5'-phosphate which are linked by a pyrophosphate bond (see Figure 1). $NADP^+$ is structurally identical to NAD^+ except for the presence of an additional phosphate group. Originally, it was proposed that $NADP^+$ contained 3 phosphate groups linked together by pyrophosphate bridges (5). Analysis of the adenylic acids release by enzymatic degradation of $NADP^+$ by Kornberg and Pricer (6) established the location of the phosphate monoester at the 2 position of the adenylic ribose. The structure of $NADP^+$ is also shown in Figure 1.

Both nucleotides possess similar redox potentials and participate in oxidation-reduction reactions which involve the reversible transfer of hydrogen at the 4 position of the pyridine ring (7-9). In most tissues, the $NADP^+$/NADPH ratio is in favor of NADPH which serves as a donor of reducing equivalents in anabolic reactions (10). The NAD^+/NADH ratio is in favor of NAD^+ which is involved in catabolic reactions and ATP-generation.

Pathways for the De Novo Biosynthesis of NAD^+

There are two major pathways for the de novo biosynthesis of NAD^+. Each pathway leads to the formation of quinolinate. Quinolinate is subsequently converted to NAD^+ via a pathway common to all organisms. In eucaryotes , tryptophan serves as the precursor for

Figure 1. Structures of NAD^+ and $NADP^+$.

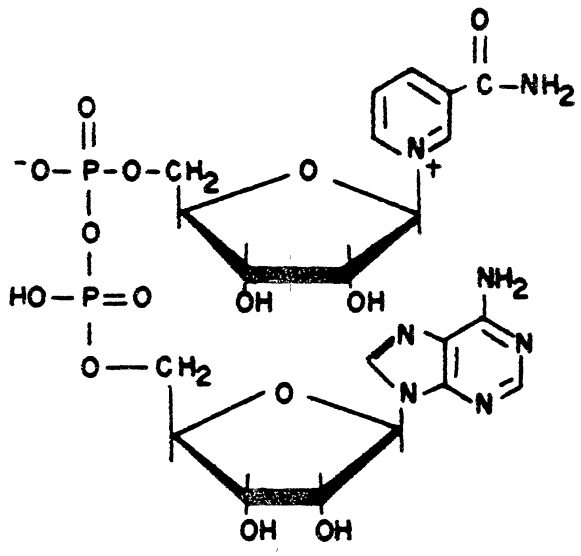

NAD$^+$

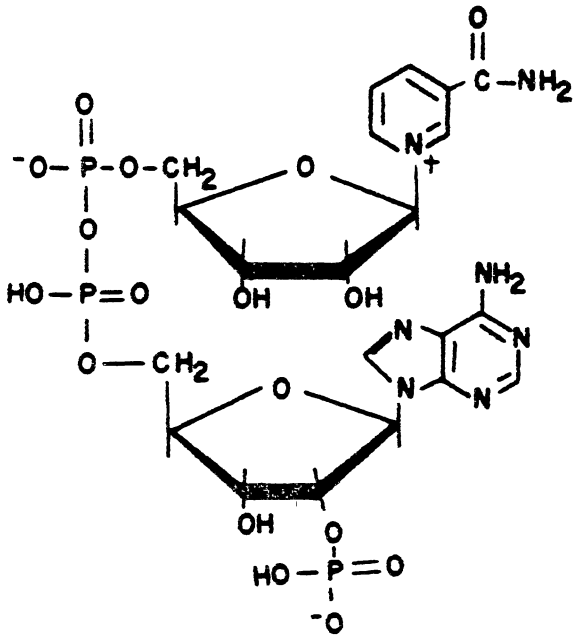

NADP$^+$

QA formation. A second pathway, found predominately in procaryotes and in some higher plants, utilizes a dicarboxylic acid and 3 carbon compound for the synthesis of QA. In addition, there exist salvage pathways by which NA, NAm, and NMN can be converted to NAD^+. The biosynthesis and degradation of NAD^+ have been extensively reviewed (11-14).

Incorporation of Quinolinate and Nicotinate into NAD^+

The role of nicotinic acid (niacin) as a nutritional supplement was demonstrated in 1937. Administration of NA and NAm relieved the symptoms of pellegra in man (15, 16) and black tongue in dogs (17). In a preliminary report (18), and later in detailed publications (19, 20), Preiss and Handler elucidated the pathway of NAD^+ formation from NA. The authors demonstrated the incorporation of ^{14}C-NA into NaMN and $dNAD^+$ in human erythrocytes. Administration of ^{14}C-NA to rats lead to the formation of labeled $dNAD^+$ before NAD^+. The reaction sequence for the synthesis of NAD^+ from NA, referred to as the Preiss-Handler pathway, has been established to be:

$$NA + PRPP \text{ ----------> } NaMN$$

$$NaMN + ATP \text{ ----------> } dNAD^+ + PPi$$

$$dNAD+ + ATP + \text{glutamine ---> } NAD^+ + AMP + \text{glutamate}$$

The first step in the reaction pathway is the formation of NaMN from NA and PRPP by nicotinate phosphoribosyltransferase. This reaction was later found to require ATP (21). The physiological Km's of the enzymes in this system and its discovery in other organisms such as yeast (22) and E. coli (23) suggested that this was the primary pathway for NAD^+ biosynthesis.

In 1963, QA was identified as a precursor of NAD^+ biosynthesis by the discovery of quinolinic acid ribosyltransferase present in E. coli and beef liver extracts (24, 25). This enzyme catalyzes the formation of NaMN by the condensation of QA and PRPP with

subsequent decarboxylation at the 2-position of QA. Thus, the pathway of NAD^+ biosynthesis de novo could be formulated as:

QA ---> NaMN ---> dNAD ---> NAD^+

QA has been established as the primary intermediate used in the de novo biosynthesis of NAD^+ whereas NA functions as an intermediate in a salvage pathway for NAD^+ formation.

Biosynthesis of NAD^+ from Tryptophan

The pathways of tryptophan metabolism have been extensively reviewed (26, 27). In 1945, Krehl et al. (28) demonstrated that tryptophan could replace the dietary requirement for niacin. Further studies showed that tryptophan administration to rats resulted in an increase in the amount of N-methylnicotinamide in the urine (28,29). Analysis of urine samples from rats given labeled tryptophan provided direct evidence of the tryptophan-niacin relationship. The labeling patterns found in isolated niacin indicated that carbon-3 of the indole ring becomes the carboxy carbon of NA (31-33) and the indole nitrogen is incorporated into the pyridine ring of NA (33, 34). Although QA had been known to be a by-product of tryptophan catabolism, it was not considered to be directly involved in NA formation (36).

3-hydroxyanthrantic acid, one of the intermediates of tryptophan degradation, is the precursor of QA. This compound can also substitute for the niacin requirement in Xanthomonas prunei (37). In 1951, Priest et al. (38) reported the presence of an enzyme which catalyzes the conversion of 3-hydroxyanthratic acid to QA. In 1963, Nishizuki and Hayashi reported the formation of NaMN from 3-hydroxyanthratic acid and PRPP in the presence of a soluble enzyme system from rat liver (36). These authors also presented evidence that free NA is not an intermediate in the conversion of 3-hydroxyanthratic acid to NaMN. 2-amino-3-acroleyl fumaric acid and QA were intermediates produced in the reaction. 2-amino-3-acroleyl fumaric acid is the primary product of the oxygenation of 3-

hydroxyanthratic acid and undergoes spontaneous cyclization to form QA (39-41). Gholson et al. (42) further demonstrated that quinolinate was an intermediate in the tryptophan to niacin pathway and showed that the enzyme forming NaMN from QA was distinct from nicotinic acid mononucleotide phosphorylase.

The NAD^+ pathway of tryptophan metabolism occurs through the following intermediates: N'-formylkynurenine, kynurenine 3-hydroxykynurenine, 3-hydroxy-anthratic acid, 2-amino-3-acroleyl fumaric acid, quinolinate, and NaMN. NaMN is subsequently converted to NAD^+ via the Preiss-Handler pathway.

QA Formation form Aspartate and DHAP

QA is also formed from L-aspartate and DHAP by the quinolinate synthetase complex. In E. coli , two gene products designated nad A and nad B have been identified in the quinolinate synthetase complex (43). The nad B protein has been purified and behaves as an L-aspartate oxidase (44). Wicks et al. (45) have demonstrated that C-3 of DHAP condenses with C-3 of L-aspartate to form QA. During the reaction of L-aspartate with the nad B protein an unstable intermediate is formed . This intermediate is believed to be iminoaspartate , since the nad B and L-aspartate requirement of the QA synthetase complex can be replaced by OAA and $NH4^+$ (46). Further support for an iminoaspartate intermediate formation came from experiments utilizing a hybrid mammalian liver-E. coli QA synthetase system. Nasu et al. (47, 48) discovered that mammalian D-aspartate oxidase could replace the E. coli nad B protein and generate QA from D-aspartate. This suggests the formation of a symmetrical intermediate which condenses with DHAP to form QA in a second reaction catalyzed by the nad A protein.

An alternative reaction for QA synthesis is found in the anaerobe Clostridium butylicum (49, 50). This bacteria condenses formate with L-aspartate to form N-formylaspartate. QA is then formed by condensation of N-formylaspartate with with acetyl-CoA.

Biosynthetic pathways for NAD^+ formation in microorganisms have been reviewed in (13).

Degradation of NAD^+

The intermediates formed in the degradation of NAD^+ can be used in salvage pathways for the resynthesis of NAD^+ (51). One of the first degradative enzymes discovered was NAD^+ pyrophosphatase which hydrolyzes the pyrophosphate linkage between the two ribose moieties of NAD^+ to yield NMN and AMP (52). The NAD^+ pyrophophatase reaction is relatively nonspecific since $NADP^+$, FAD, and ATP also function as substrates (53). In eucaryotes, NMN formed by the action of NAD^+ pyrophosphatase can be utilized to form NAD by NMN adenyltransferase (14). In procaryotes, NMN can be deaminated to form NaMN which can be converted to NAD^+ via the Preiss-Handler pathway (13).

A second mechanism for NAD^+ degradation is cleavage of the N-glycosidic bond of the oxidized nucleotide by NAD^+ glycohydrolase to form NAm and ADPR. This enzyme was first discovered in mammalian tissues by Handler and Klein (54) and is widely distributed in many organisms (55). NAD^+ glycohydrolases present in microorganisms and Bungaris fucalius venom are soluble proteins, whereas mammalian NAD^+ glycohydrolases are membrane-bound with the exception of the enzyme found in bull semen (56, 57). A heat-labile protein inhibitor of NAD^+ glycohydolases in Mycobacterium butyricum (58-61) and Pseudomonas putudi (62) has also been described.

NAm liberated by the hydrolysis of NAD^+ can be recycled to form NAD^+. It is generally believed that NAm is deaminated to form NA which is incorporated into NaMN by NA phosphoribosyltranferase, although direct mechanisms for NMN formation from NAm have been demonstrated (63, 64).

A unique feature of mammalian NAD^+ glycohydrolases is the ability to catalyze a pyridine base exchange reaction with NAD^+. Utilizing ^{14}C-labeled NA, Zatman et al. demonstrated that the label could be incorporated into intact NAD^+ (65). This reaction is

relatively nonspecific for pyridine derivatives and has been used to prepare a number of NAD^+ analogs (66). A general mechanism is presented below:

NAmADPR + X ----------> XADPR + NAm

In the case of NAD^+ hydrolysis, the acceptor X is H_2O, whereas in the base exchange reaction X represents a pyridine base.

Although free NAm produced by NAD^+ hydrolysis can be recycled via a salvage pathway, the true physiological role of NAD^+ glycohydrolase in pyridine metabolism remains unclear. Kaplan has suggested that the enzyme regulates the levels of free NAD^+ in the cell with enzyme-bound NAD^+ being less susceptible to hydrolysis (67). However, experimental evidence in support of this hypothesis is contradictory (68, 69) and enzyme-bound NAD^+ may only partially account for NAD^+ glycohydrolase regulation of coenzyme levels. Figure 2 summarizes the pathways of NAD biosynthesis and degradation.

Biosynthesis of $NADP^+$ by NAD^+ Kinase

The synthesis of $NADP^+$ from NAD^+ was first demonstrated in crude yeast extracts by Vestin in 1937 (70). Further confirmation of this finding by Von Euler and Adler in 1938 showed that $NADP^+$ formation in this system required ATP (71). In 1948, Mehler, Kornberg and others identified a similiar reaction in pigeon liver homogenates (72). The observations made in both systems suggested that $NADP^+$ is synthesized by an ATP-dependent phosphorylation of NAD^+. Kornberg later described the partial purification of the kinase catalyzing the formation of $NADP^+$ in yeast (73). Other reports quickly followed on the purification of similar kinases from the tissue of rabbits (74) and pigeons (75).

NAD^+ kinase catalyzes the direct phosphorylation of NAD^+ by ATP in the final step of $NADP^+$ biosynthesis. This reaction is specific for the B-anomer of NAD^+, however, Suziki et al. (76) have reported the presence of a specific a-NAD^+ kinase for the synthesis of a-$NADP^+$ in Azotobacter vinelandii. In addition, NADH kinases have been identified in the mitochondria of brewer's (77) and baker's yeast (78, 79).

Figure 2. Biosynthetic Pathways for the Synthesis of the Pyridine Nucleotides.

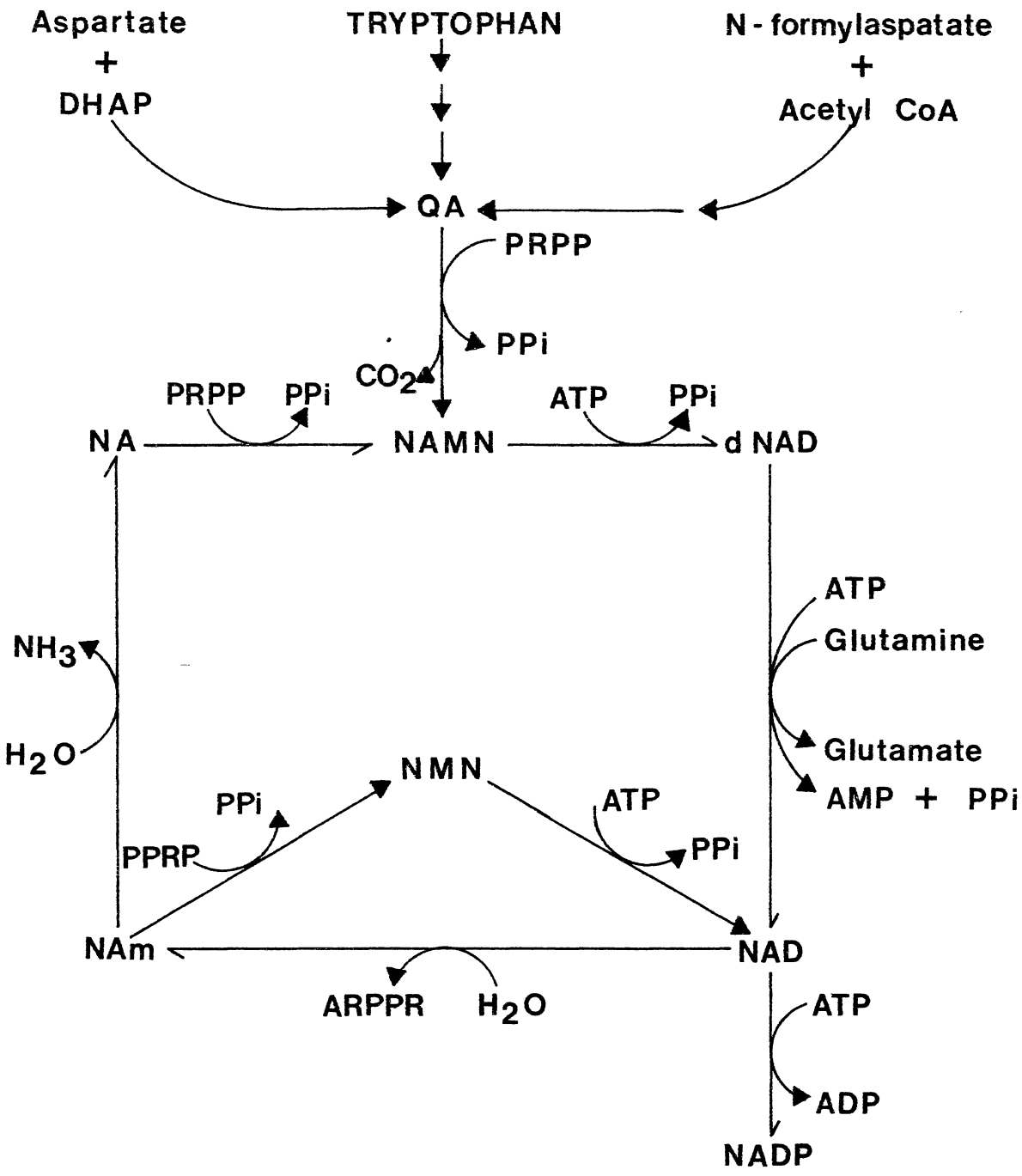
Aspartate
+
DHAP
TRYPTOPHAN
N - formylaspatate
+
Acetyl CoA
QA
PRPP
PPi
CO2
PRPP
PPi
ATP
PPi
NA
NAMN
d NAD
ATP
Glutamine
NH3
H2O
Glutamate
AMP + PPi
NMN
PPi
PPRP
ATP
PPi
NAm
NAD
ARPPR
H2O
ATP
ADP
NADP

The exact mechanism for the formation of NAD^+ from $NADP^+$ is unknown. The conversion of $NADP^+$ to NAD^+ has been observed in extracts of yeast (71) and potatoes (73). Katchman et al. have described NAD^+ formation from $NADP^+$ by the cyclophorase system in rabbit liver and kidney (74). Alkaline phosphatase can also hydrolyze $NADP^+$ to NAD^+, however, the reaction rate is much lower with $NADP^+$ than with other substrates (80). An acid phosphatase capable of converting $NADP^+$ to NAD^+ and NADPH to NADH has been partially purified from pea leaves (81). This reaction is relatively nonspecific since this enzyme attacks a number of different substrates. At this writing, there is no direct evidence of an $NADP^+$-specific phosphatase. The conversion of $NADP^+$ to NAD^+ may be mediated by a combination of nonspecific phosphatases.

Purification of NAD^+ Kinase

The majority of NAD^+ kinases studied thus far are soluble proteins of cytoplasmic origin (82). In addition to soluble NAD^+ kinases in these systems, some NAD^+ kinase activity is reported to be associated with the mitochondrial fraction in yeast (83) and rat liver (84). NAD^+ kinase activity has also been reported in the nuclear fraction isolated from rat brain and dog thyroid (85). NAD^+ kinase in plants is present in the cytoplasm and inside the chloroplasts. The results of Muto et al. (86) demonstrate that virtually all the NAD^+ kinase activity in wheat, sunflower, crabgrass, and foxtail is present in the chloroplasts, whereas in peas and corn, only 70% and 5% is recovered in this fraction, respectively. In spinach leaf, NAD^+ kinase activity is located in the soluble portion of the cell components and less than 5% is located in the chloroplasts (87). Dieter and Marme have described a Ca^{++}/calmodulin-dependent NAD^+ kinase located in the outer mitochondrial membrane of corn (88). Table I summarizes the various sources from which NAD^+ kinase has been isolated and purified.

Most purification procedures have many similarities. Virtually all procedures utilize ammonium sulfate fractionation and most contain a DEAE-cellulose step. Calcium

TABLE I

REPORTED PURIFICATIONS OF NAD^+ KINASE FROM VARIOUS SOURCES

Sources	Tissue	Reference(s)
Animal		
Rat	Liver	92, 93, 94
	Brain	95
Pigeon	Heart	96, 97, 98
	Liver	94, 75
Rabbit	Liver	74, 100
	Skeletal	101, 102
Human	Neutrophils	90
Sea Urchin	Eggs	103, 104
Plants		
Corn		88
Spinach	Leaves	87
Peas		105, 106
Yeast		
Candida utilis		89
Sacchromyces cerevisiae		73, 107, 108
Fungi		
Neurospora crassa		109
Bacteria		
Azotobacter vinellandi		110

phosphate gels and protamine sulfate are also frequently used in the initial stages of purification.

In recent years, affinity chromatography has been employed during the final stages of purification. Immobilized triazine dyes have been particularily useful in purifying NAD^+ and $NADP^+$ requiring dehydrogenases and certain kinases through interaction with the nucleotide-binding domains of the enzymes. Blue sepharose has been used to purify Candida utilis NAD^+ kinase (89). Procion Red-agarose, which is more specific for $NADP^+$-linked enzymes, has been used in the purification of a calmodulin-dependent NAD^+ kinase from human neutrophils (90). Calmodulin-dependent NAD^+ kinase from plants has also been purified by affinity chromatography on calmodulin-Sepharose (91).

Only a semiquantitative comparison can be made between many of the listings in Table I. Different assay procedures were used and the reaction rate is dependent on the conditions of the assay such as pH, ionic strength, unintended inhibitors or activators, side reactions, temperature, and possibly the concentration of the enzyme. The specific activity will also be dependent on the method of protein estimation.

Molecular Weight of NAD^+ Kinases

NAD^+ kinase is thought to be a large, multimeric enzyme complex. A molecular weight of 270,000 has been reported for pigeon liver NAD^+ kinase (111). Analysis of the purified enzyme by SDS-PAGE revealed a single protein component with a molecular weight of 34,000. This suggests the native enzyme may be an octomer of identical subunits.

Tseng et al. have proposed a tetrameric structure for S. cerevisiae NAD^+ kinase based on the molecular weight of the native enzyme of 124,000 with subunits of 34,000 (108). A similar subunit molecular weight of 32,000 is seen for the NAD^+ kinase of C. utilis with a native molecular weight of 260,000 (89).

NAD^+ kinases from rabbit skeletal muscle (100, 112) and pigeon heart (115) appear to have multiple active forms. The molecular weight of the skeletal muscle enzyme ranges from 31,000 to 370,000, whereas, pigeon heart NAD^+ kinase has a variable molecular weight of 90,000 to 270,000. NAD^+ kinase from rabbit liver also exists in multiple forms composed of subunits of 34,000 daltons and 62,000 daltons (100). Table II summarizes the molecular weights of NAD^+ kinase that have been reported.

Divalent Cations

A divalent metal cation is an absolute requirement for NAD^+ kinase in all cases studied, with Mg^{++} being the most effective. As with a number of other kinases, Mg^{++} chelates anionic ATP and the MgATP complex is the actual substrate for the phosphorylating reaction (117). In addition to Mg^{++}-ATP, NAD^+ kinase also shows activity with other divalent metal-ATP complexes in pigeon liver (73) and rat liver (92). In rat liver, the order of effectiveness of metal substitution was $Mg^{++} > Mn^{++} > Zn^{++} > Fe^{++} > Ca^{++} > Co^{++}$. No activity was found with Ba^{++}, Sn^{++}, Ni^{++}, Cu^{++}, or Fe^{+++}. In spinach leaves, Co^{++} can replace Mg^{++} at the same concentration with 50% of the activity (87). Mn^{++}, Zn^{++}, Ni^{++}, and Ca^{++} show negligible replacement activity.

In sea urchin eggs, Mn^{++} is stimulatory at concentrations of 0.5 mM (103). Above this range, however, Mn^{++} is inhibitory. This inhibition could not be prevented by the addition of 10 mM Mg^{++}.

The most extensive studies on the effects of metal-ATP complexes on NAD^+ kinase are with the pigeon liver enzyme (118). This enzyme is activated by Mg^{++}, Co^{++}, Mn^{++} and Zn^{++}, the optimum metal-ion ATP ratio being 3.0, 2.0, 0.8, and 0.5 respectively. Metal-ions added in excess over the optimum ratios are inhibitory. The difference in response to various activating ions resides in changes in the Km for each metal-ion complex, with V_{max} and KmNAD being unaffected. The enzyme is also inhibited by free Mg^{++} and ATP.

TABLE II

MOLECULAR WEIGHTS OF ISOLATED NAD^+ KINASES[a]

Source	Molecular Weight	Reference(s)
Liver		
Pigeon	270,000	111
Rat	250,000	94
Rabbit	180,000-650,000	100
	136,000	98, 110
Chicken	275,000	113
Neutrophils		
Human	169,000	90
Muscle		
Rabbit skeletal	40,000, -300,000	114
Pigeon heart	90,000, 270,000	115
Plant		
Squash	~50,000	116
Yeast		
C. utilis	260,000	89
Fungi		
S. cerevisiae	124,000	108
Neurospora crassa	203,000-338,000	109
Bacteria		
A. vinellandii	130,000	110
Marine		
Sea Urchin Eggs	310,000	103, 104

[a]Reference (113).

Inhibition

Wang and Kaplan first reported inhibition of NAD^+ kinase from pigeon liver by NADH with a Ki of 0.9 mM (75). Apps (99) reported values for Ki of 0.09 mM and 0.04 mM for NADH and NADPH, respectively with NAD^+ kinase from the same source. Ki values of 0.1 mM for NADH and 0.05 mM for NADPH were determined for the rat liver enzyme (93). Sea urchin egg NAD^+ kinase has a Ki for NADH of 0.33 mM and Ki of 0.13 mM for NADPH. In all cases, the reduced nucleotides were competitive with NAD^+, with NADPH appearing to be a more potent inhibitor. In rat brain, NADH is also an inhibitor of the enzyme; however, NADPH has no effect (95). These findings have lead to the suggestion that the levels of reduced nucleotides could be an important factor in controlling NAD^+ kinase activity and resulting $NADP^+$ levels.

Apps has demonstrated that NADPH is also a competitive inhibitor with Mg-ATP (99). This finding suggested that the g-phosphate of ATP is normally bound near the 2'-hydroxyl of NAD^+ and that the competitive inhibition could occur by NADPH overlapping this binding site. The kinetic data of Apps suggests the presence of two classes of interacting NAD^+-binding sites on pigeon liver NAD^+ kinase (111). The main limiting factor, however, may be changes in the hepatic ATP concentrations. In the presence of invariant ATP concentrations, control might be exercised by changes in the levels of NADPH. The presence of NAD^+ binding sites with differing affinities has not been demonstrated with NAD^+ kinase from other sources.

Mechanism

Initial velocity studies have been performed on the C. utilis enzyme (119). An intersecting pattern was obtained with replots of the slope and intercept linear. Computer analysis of the data indicates both C. utilis and chicken liver NAD^+ kinase follow a sequential mechanism of addition of reactant (NAD^+ and ATP) binding before product is

released. Product inhibition studies with ADP at low concentrations of fixed substrates gave rise to noncompetitive patterns with parabolic slope and intercept replots. When the concentration of fixed NAD^+ is raised to 80 mM, noncompetitive inhibition is seen with parabolic slope and linear intercept replots. When the fixed ATP levels are raised to 40 mM, linear noncompetitive inhibition occurs. These findings have been considered in formulating a rapid equilibrium random mechanism proposed in Scheme 1, Figure 3. This scheme depicts the random addition of ATP and NAD^+ to the enzyme and multiple binding of ADP to the free enzyme and the E.NAD^+ and E.ATP complexes where NAD^+, ATP, and ADP are designated A, B, and I, respectively.

Support for this scheme is seen in the slope parabolic-intercept linear noncompetitive inhibition observed with high levels of ADP at the 80 mM concentration of NAD^+ in which the enzyme inhibitor complexes EAI, EAI2 and EBI are predominant.

A rapid equilibrium random addition is also proposed for pigeon liver NAD^+ kinase (99). An intersecting initial velocity pattern was seen for both NAD^+ and ATP. Inhibition by ADP was competitive with ATP and noncompetitive with NAD^+. Conversely, NADH was competitive with NAD^+ and noncompetitive with ATP. NADPH was competitive with both NAD^+ and ATP; however, the inhibition is not strictly competitive with ATP suggesting that the binding of ATP is reduced but not prevented.

The rapid equilibrium random mechanism for pigeon liver NAD^+ kinase is seen in Scheme 2, Figure 3. This scheme is supported by the type of inhibition produced by NADH and ATP. In both cases, the inhibition is noncompetitive toward the other substrate. Furthermore, the competitive inhibition produced by NADPH is incompatible with an ordered addition mechanism. Further studies on the product inhibition of pigeon liver NAD^+ kinase have resulted in a revision of the product inhibition of ADP versus NAD^+ to competitive inhibition (120).

Orringer and Chung have proposed a ping-pong mechenism for A. vinelandii NAD^+ kinase (121). Parallel line kinetics are observed with varying NAD^+ concentrations at

Figure 3. Schematic Diagrams of the Reaction Mechanisms of NAD^+ Kinase.

a) C. utilis

b) Pigeon Liver

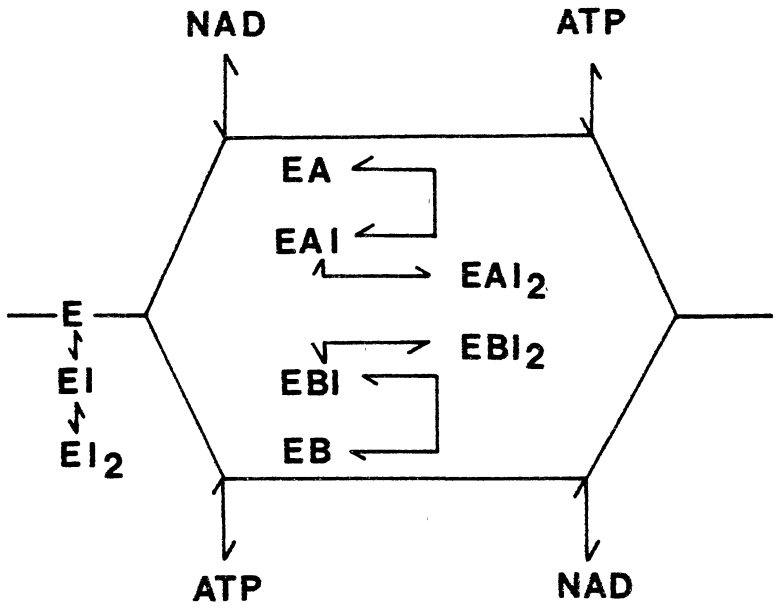

a) Scheme 1

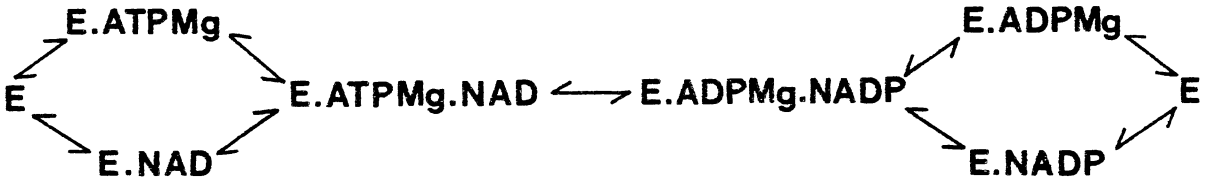

b) Scheme 2

different fixed concentrations of ATP. Product inhibition kinetics demonstrated that ADP was noncompetitive with ATP and competitive with NAD^+. However, $NADP^+$ was noncompetitive with ATP. The enzyme also catalyzes an exchange reaction between ^{14}C-ADP and ATP. Experiments with varing concentrations of NAD^+ and a constant concentration of ADP indicate that the exchange rate decreases with an increasing concentration of NAD^+. This observation suggests that $NADP^+$ production from NAD^+ and ATP and the exchange reaction proceed through a common enzyme intermediate. Nicotinamide 2-deoxyadenine dinucleotide ($NdAD^+$), a non phosphorylatible inhibitor of NAD^+ has been utilized in inhibition studies with pigeon liver NAD^+ kinase (122). Inhibition by $NdAD^+$ was competitive with NAD^+ and noncompetitive with ATP. A similar pattern was obtained with the reduced form of the analog. The similarities between the Ki of $NdAD^+$ and Km of NAD^+ and the Ki's of $NdAD^+$ and NADH suggest that the 2' hydroxyl is unimportant to the binding of NAD^+ and NADH to the enzyme.

Modifications

Protein modifying reagents have been used to probe the active site of NAD^+ kinase. All available evidence to date suggests that sulfhydryl groups play a critical role in the manifestation of the enzyme's activity. The NAD^+ kinases of pigeon heart (96) and rat liver (93) are susceptible to inhibition by hydroxy mercuribenzoate (HMB). This inhibition is reversed by addition of L-cysteine and B-mercaptoethanol. Pigeon heart NAD^+ kinase is also inhibited by N-ethyl maleimide (NEM) (96). Preincubation of the enzyme with NAD + ATP partially protected the enzyme from inactivation.

Pigeon liver NAD^+ kinase is susceptible to alkylation by 3-bromo-acetyl-pyridine (BAP) (123). Mn^{++}-ATP and NAD^+ protect the enzyme, whereas NADH, Mn^{++} and ATP increase the rate of inactivation.

It has been shown that BAP inactivates the enzyme first by the rapid modification of two or more groups to form a partially active species, then by the slow alkylation of a third

residue producing complete inactivation (124). Both NAD^+ and Mn^{++}-ATP protect the enzyme from BAP, whereas NADH, ATP, and Mn^{++} increase the rate of inactivation. Further studies on the reaction with BAP suggests the alkylation of a group not necessarily involved in catalysis, but in NAD^+ binding. In the absence of direct amino acid analysis, the true identity of the groups inactivated in the enzyme is uncertain.

Photoinactivation of pigeon heart NAD^+ kinase occurs in the presence of the dye sensitizers, methylene blue and bengal rose (125). The addition of NAD^+ and ATP does not prevent the inactivation of the enzyme. Differential UV-spectra of the native enzyme and the photoinactivated enzyme correlated with the loss of catalytic activity suggest that the loss of catalytic activity is due primarily to modification of the histidine residues. Sulfhydryl groups are also oxidized during photoinactivation with a subsequent loss of activity.

Regulation of NAD^+ Kinase

The level of NADP+ within cells is generally lower than NAD^+, although the size of the $NADP^+$ pool varies in different cell types. The level of $NADP^+$ within the cell may be related to amounts of $NADP^+$-linked dehydrogenases present (67, 126). Administration of NAm to mice leads to a 10-fold increase in the concentration of the liver pyridine nucleotides (127). However, only a small amount of the newly-generated nucleotides is $NADP^+$.

The isotope studies of Stollar and Kaplan (128) indicate that there is a slow equilibrium between the pools of NAD^+ and $NADP^+$. Administration of labeled phosphorus demonstrated that the oxidized and reduced forms of the nucleotides are in rapid equilibrium, whereas the internal phosphates between NAD^+ and $NADP^+$ were slowly exchanged. This finding indicated a slow equilibration between the pools of NAD^+ and $NADP^+$. However,the phosphate group at the 2' hydroxyl is turned over at a rapid rate which suggests the presence of a mechanism for the hydrolysis of this group followed by

rephosphorylation by NAD^+ kinase. Such a mechanism may have an important role in regulating $NADP^+$ levels with respect to the concentration of NAD^+.

Dietrich and Yero have found that the injection of NAm raises hepatic NAD^+ levels, but decreases hepatic ATP (129). Clark and Greenbaum have suggested that differing levels of NAD^+ and $NADP^+$ seen after NAm injection may occur by competition for available ATP by enzymes synthesizing NAD^+ and $NADP^+$ (130).

Hormonal Regulation

Incubation of dog thyroid tissue slices with thyroid stimulating hormone (TSH) increases the level of $NADP^+$ and NADPH with a concomitant decrease in NAD^+ concentration (131). Field and coworkers (132) have suggested that the high levels of $NADP^+$ may be brought about through stimulation of NAD^+ kinase. New protein synthesis was not involved since puromycin did not inhibit the response to TSH (133).

Greenbaum, Clark, and McClean have studied the effects of different hormonal conditions on the level of pyridine nucleotides in rat liver. Adrenalectomy, glucagon administration, and growth hormone administration decreased the $NADP^+$ content in the liver. However, there appears to be little correlation between the activity of NAD^+ kinase and the $NADP^+$ concentration (134, 135). Greenbaum and co-workers have noted that NAD^+ kinase in both rat liver and rat mammary gland appears to have a potential activity greatly exceeding the actual rate of synthesis of $NADP^+$ and may be regulated by the availability of ATP.

Circadian Rhythms

Some eucaryotic microorganisms display circadian metabolic rhythms similar to those found in higher plants and animals. Investigations into these rhythms in the duckweed Lemna gibba G3 and Euglena have suggested that the cyclical variations in the levels of NAD^+ and $NADP^+$ may constitute a self-sustaining oscillatory loop (136). These studies

have led to the development of a hypothetical model in which increases in the levels of NAD^+ enhance the rate of Ca^{++} efflux from the mitochondria into the cytoplasm with a maximal concentration of cytoplasmic Ca^{++} occurring after 6 hours. Ca^{++} would activate a Ca^{++}/calmodulin-dependent NAD^+ kinase and inhibit $NADP^+$ phosphatase leading to a decrease in the net production of NAD^+ with a maximal rate of $NADP^+$ production 12 hours later. This process would lead to a minimum level of NAD^+ occuring 6 hours later after which NAD^+ production would resume. Concurrently, Ca^{++} not bound to calmodulin would be taken up by the mitochondria and $NADP^+$ phosphatase would be slowly released from inhibition for the formation of NAD^+ from $NADP^+$.

Although this model attempts to explain only a part of the complex metabolic interactions which constitute circadian rhythms, the existence of such a mechanism is only postulated and still requires experimental verification.

Role of NAD^+ Kinase in Development

One of the earliest events seen in the fertilization of sea urchin eggs is a transient increase in concentration of free cytoplasmic Ca^{++} due to the release of this ion from intracellular stores (137, 138). Concurrently, there is an elevation of NADPH levels in the cell (139). This elevation is due to activation of NAD^+ kinase during the first 90 seconds after insemination and results in the conversion of one-quarter of the cell's NAD^+ into $NADP^+$ and NADPH (140). The increase in NADPH concentration occurs through the reduction of $NADP^+$ by the enzymes of the hexose monophosphate pathway.

The relationship between the increase in Ca^{++} levels and the activation of NAD^+ kinase was established by Epel and co-workers who demonstrated the regulation of sea urchin NAD^+ kinase by calmodulin (141). In this system, NAD^+ kinase is activated by less than μM amounts of Ca^{++} and a heat-stable activator that can be disassociated from the enzyme with a resulting loss of activity. The physical properties of the activator correspond closely with bovine brain calmodulin. The stimulation of NAD^+ kinase is inhibited by

trifluoperazine, a known inhibitor of calmodulin. A calmodulin-sensitive NAD^+ kinase has also been found in the eggs of the amphibian Pleurodies waltii (142) and starfish oocytes (143).

Sea urchin NAD^+ kinase is also subject to activation by limited proteolysis, a property which is common among other calmodulin-dependent enzymes (144). This activation is accompanied by a loss in Ca^{++} sensitivity and suggests that these enzymes interact with calmodulin in a similar manner.

NAD^+ Kinase in Neutrophils

Superoxide production by NADPH oxidase in activated neutrophils is generally believed to be reponsible for the destruction of invading bacteria (145). As a particle is phagocytosed, membrane-bound NADPH oxidase fuses with a phagocytotic vesicle and produces superoxide. NADPH required for this reaction is produced by the hexose monophosphate pathway. $NADP^+$ is a rate-limiting factor for glucose-6-phosphate dehydrogenase which controls the rate of glucose oxidation by this pathway (146).

Although the hexose monophosphate shunt is thought to be driven by production of $NADP^+$ from NADPH by NADPH oxidase, Sparkman et al. have suggested the total pool of $NADP^+$ and NADPH may be insufficient for the production of superoxide and that an increase in the levels of $NADP^+$ is required for optimal NADPH oxidase activity (147). These investigators demonstrated a 2-3 fold increase in the total pool size of $NADP^+$ and NADPH upon activation of human neutrophils. This increase could be blocked by the addition of calcium and calmodulin antagonists. A Ca^{++}/calmodulin sensitive NAD^+ kinase has been isolated from human neutrophils (90). Based on these findings, the increase in the the activity of the hexose monophosphate shunt in activated neutrophils may be due to the enhanced production of $NADP^+$ by calmodulin stimulated NAD^+ kinase.

Regulation of Plant NAD^+ Kinase

Yamamoto has suggested that the rate-limiting factor in the metabolism of plants is both NAD^+ and $NADP^+$ (148). $NADP^+$ and NADPH levels are high in the growing portion of plants, whereas NAD^+ and NADH predominate in the storage organ. In young plants, the NADPH/$NADP^+$ ratio is high; however, this ratio decreases with the age of the tissue.

In studying the pyridine nucleotide levels in Chlorella, Oh-Hama and Miyachi discovered the quantitative conversion of NAD^+ to $NADP^+$ upon illumination (149, 150). This light-induced conversion also takes place within the chloroplasts of higher plants (151). Muto et al. have described the presence of NAD^+ kinase within intact chloroplasts and propose that the light-induced conversion of NAD^+ to $NADP^+$ is the result of photoactivation of NAD^+ kinase (86).

NAD^+ kinase in higher plants is stimulated by an activator molecule which is disassociated from the enzyme by passage through DEAE-cellulose (152). This activator is susceptible to proteolytic digestion, highly acidic, and relatively heat-stable. The stimulation of plant NAD^+ kinase was later shown to be Ca^{++}-dependent and the activator was analgous to calmodulin in its ability to stimulate cyclic nucleotide phosphodiesterase (153).

The activator was subsequently identified as plant calmodulin and shares similar properties with animal calmodulin including molecular weight, electrophoretic mobility, and inhibition by phenothiazine drugs (154). Fungal and yeast calmodulins can also activate pea NAD^+ kinase, as well as calmodulin isolated from slime mold Disctyostelium discoideum (155, 156). However, plant and animal calmodulin are not equally active in the stimulation of plant NAD^+ kinase. Peanut seed calmodulin is about seven-fold more active than porcine brain calmodulin in the stimulation of the plant enzyme (157). Subtle

variations in the amino acid sequence between the two calmodulins may account for the difference in their abilities to activate plant NAD^+ kinase.

Plant NAD^+ kinase is almost totally dependent on Ca^{++} and calmodulin for its enzymatic activity (158). In addition, there is a 10-fold molar excess of calmodulin over NAD^+ kinase in pea seedling extracts (159). Corimer and co-workers indicate that calmodulin-activated NAD^+ kinase is the major form of NAD^+ kinase in pea seedlings (160).

Corimer has presented a model for the light-induced conversion of NAD^+ to $NADP^+$ based on the activation of Ca^{++}/calmodulin-dependent NAD^+ kinase (160). This model is seen in Figure 4.

A key feature of this model is a photoreceptor-mediated increase in Ca^{++} concentration from a resting level of 10-7-10-8 M to 10-5-10-4 M upon illumination. This Ca^{++} increase would promote the formation of active Ca^{++}-calmodulin complexes. The presences of such active complexes would activate NAD^+ kinase for the conversion of NAD^+ to $NADP^+$.

There are two lines of evidence which support the existence of the model in vivo. Muto et al. have demonstrated the rapid accumulation of Ca^{++} ions inside chloroplasts upon illumination (161). These investigators suggest that stromal free Ca^{++} is regulated between 10-7 to 10-5 M which is similar to the cytoplasmic free Ca^{++} levels seen in eucaryotes.

A second line of evidence has been the discovery of a calmodulin-like molecule within the stroma of pea chloroplasts (162). Incubation of pea protoplasts with calmodulin-inactivating drugs inhibited the light-induced conversion of NAD^+ to $NADP^+$ at concentrations which inhibit calmodulin-dependent enzymes. These findings suggest that the light-induced conversion of NAD^+ to $NADP^+$ coupled to the activation of NAD^+ kinase by calmodulin may actually operate in vivo.

Figure 4. Model for the Activation of Plant NAD^+ Kinase by Calmodulin. See Reference 160.

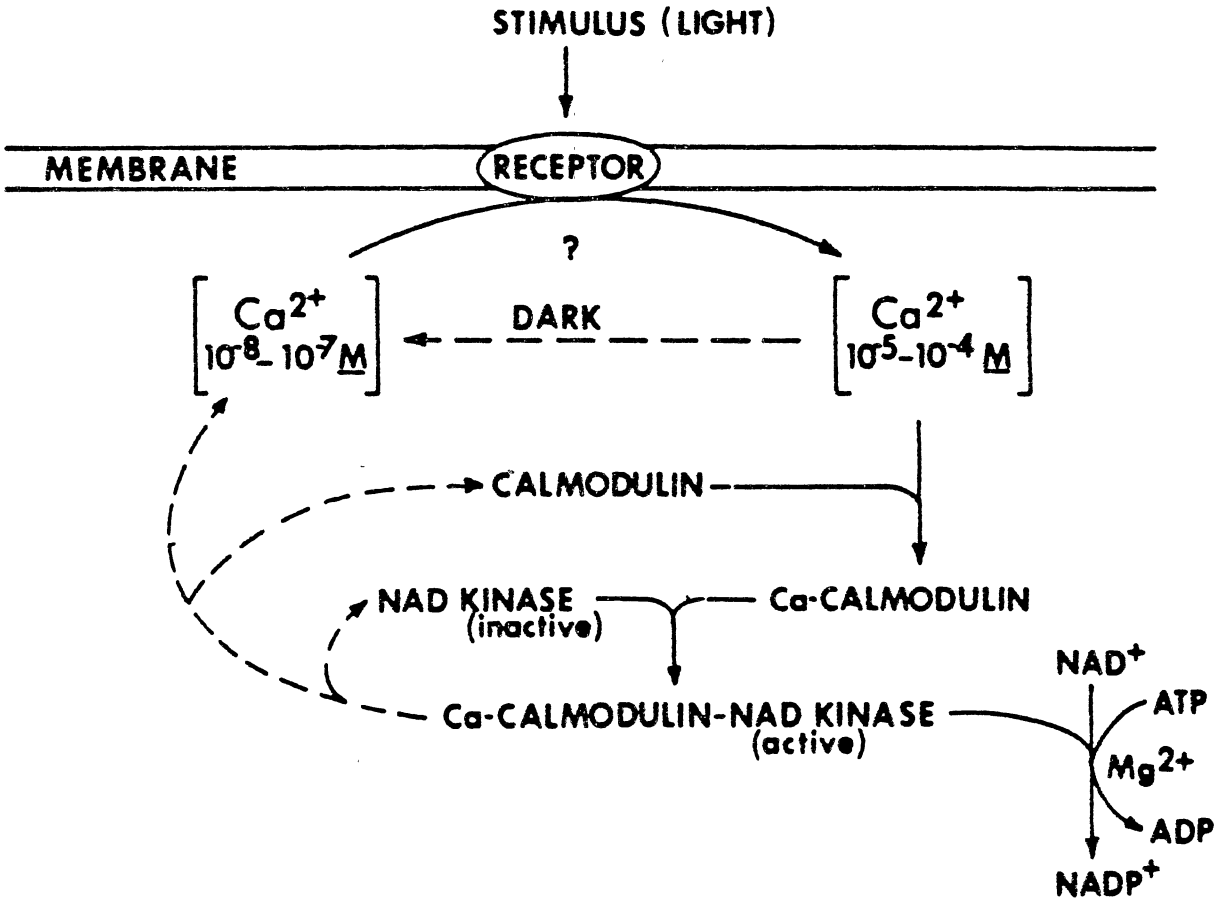
STIMULUS (LIGHT)
MEMBRANE
RECEPTOR
?
Ca^{2+} 10^{-8}–10^{-7} M
DARK
Ca^{2+} 10^{-5}–10^{-4} M
CALMODULIN
NAD KINASE (inactive)
Ca-CALMODULIN
Ca-CALMODULIN-NAD KINASE (active)
NAD^+
ATP
Mg^{2+}
ADP
$NADP^+$

CHAPTER III

MATERIALS AND METHODS

Animals

The rats used in this study were purchased from Charles River Breeding Laboratories, Massachusetts or obtained from a colony maintained by Lab Animal Resources, Oklahoma State University. The strains of rats used were either Fischer-344 or Holtzmann. All rats were maintained on a diet of Wayne Lab-Blox and water ad libitum. The animals were fasted overnight prior to sacrifice.

Spectrophotometric Assay for NAD^+ Kinase

NAD^+ kinase was assayed by quantitating the amount of $NADP^+$ synthesized by the enzyme by reduction of $NADP^+$ to NADPH using isocitrate dehydrogenase in a discontinuous assay as previously described (92). Assays were performed in a 0.5 ml final volume and contained 10 mM NAD^+, 13 mM ATP, 10 mM $MgCl_2$, 10 mM sodium pyruvate, 10 mM nicotinamide, and 0.350 M Tris-HCl, pH 8.0. The reaction was initiated by an aliquot of enzyme. The reaction mixtures were incubated at 37°C for the appropriate time intervals and terminated by heating in a boiling water bath for 1 minute. The reactions were then cooled on ice and centrifuged for 10 minutes in a Damon clinical centrifuge. Reaction time intervals of 0, 10, 20, and 30 minutes or 0, 15 and 30 minutes were commonly used.

For quantitating the amount of $NADP^+$ produced with the reaction mixtures, 0.3 ml of the assay supernatant was placed in a 1 ml quartz cuvette. Approximately 0.7 ml of 0.05 M Tris-HCl, pH 8.0 and 20 ul of isocitrate dehydrogenase (200 units/ml) were added and the

initial absorbance at 340 nm was recorded. A 0.05 ml aliquot of 0.05 M isocitrate was then added and the solution within the cuvette was gently mixed. A final absorbance reading was taken when no further increase in the absorbance was seen. A unit of enzyme activity is defined as the amount of enzyme that can form 1 micromole of $NADP^+$ from NAD^+ per hour at 37°C in the assay system used. The calculation of units was carried out as follows:

$$\text{units} = \frac{A_2 - A_1}{t_2 - t_1} \times 17.2$$

where A_2 and A_1 denote the change between the initial and final absorbance reading at each respective time interval t_2 and t_1.

Nicotinamide and sodium pyruvate were included in the enzymatic assays through the early stages of purification of NAD^+ kinase. These compounds could be omitted from the reaction mixtures after the DEAE-Biogel A step since the presence or absence of the compounds at this stage had no effect on NADP synthesis.

HPLC Assay of NAD^+ Kinase

For inhibition studies with NADH, NADPH, $NADP^+$, and 3-acetyl pyridine adenine dinucleotide (APAD), the activity of NAD^+ kinase was measured by the synthesis of ^{14}C-$NADP^+$ using a modification of the assay decribed by Oka and Field (93). Reaction mixtures contained 0.5 mM ^{14}C-NAD^+ (specific activity - 0.75 μCi/μmol) 5 mM MgATP, 5 mM $MgCl_2$, 150 mM N-ethylmorpholine, pH 8.0, and varying concentrations of the inhibitors in a final volume of 0.45 ml. The reactions were initiated by the addition of 50 μl of enzyme and incubated for 30 minutes at 37°C. The reactions were then terminated by heating in a boiling water bath for 1 minute and centrifuged for 10 minutes.

In order to avoid the tedious procedure of separating the reaction components by Dowex chromatography, a rapid separation procedure was developed using reverse-phase HPLC. Components of the reaction mixtures can be separated on a 25 cm long RP-18 (10

micron) column using a linear gradient from 0.5% to 2.0% acetonitrile in 0.01 M ammonium phosphate, pH 5.5. The HPLC unit consisted of 2 Waters Model M-45 pumps, a Waters Model 660 solvent programmer, and a Gilson Model 201 programmable fraction collector. Absorbances of the eluting compounds was detected at 254 nm using a Waters Model 440 detector. The flow rate was 2 ml/min. with a pressure of 1750 psi. The time differential between the initial and final conditions of the gradient was 10 minutes. A representative elution profile appears in Figure 5a. The average retention times of each compound run separately was: MgATP - 1.8 min.; MgADP - 2.3 min.; $NADP^+$ - 3.8 min.; NADPH - 6 min.; NAD^+ - 9.8 min.; and NADH - 9.8 min. The elution of NAD^+ and NADH from the column are virtually identical using this procedure. Figure 5b contains a similar elution pattern as that of Figure 5a, with the addition of APAD (average retention time - 12.4 min).

In order to determine the amount of ^{14}C- $NADP^+$ synthesized, a 0.05 ml aliquot of each reaction mixture was added to 0.9 ml of 0.5% acetonitrile, 0.01 M ammonium phosphate, pH 5.5. A 0.05 ml spike of 2.0 mM $NADP^+$ was added, making the final dilution 1 to 20. A 500 µl aliquot of this sample was then injected onto the column. Fractions of 5 ml containing the $NADP^+$ peak were collected using the program-time mode of the fraction collector. Determination of ^{14}C-labeled $NADP^+$ was carried out by counting a 1 ml aliquot of each 5 ml fraction with 10 ml of Insta-Gel using a liquid scintillation counter. The samples were counted for 5 minutes each and the counts per minute were converted to disintegrations per minute by the external sample channels ratio method and background subtraction. The net dpm values for each 5 ml fraction was calculated after correcting for any ^{14}C NAD^+ appearing in the $NADP^+$ peak and the recovery of $NADP^+$ from the column. The recovery of $NADP^+$ from the column was 67.5%.

Figure 5. HPLC Elution Profile of the Pyridine and Adenine Nucleotides.

Peak No.	Nucleotide
1	MgATP
2	MgADP
3	$NADP^+$
4	NADPH
5	NAD^+ + NADH
6	APAD

See text for experimental details.

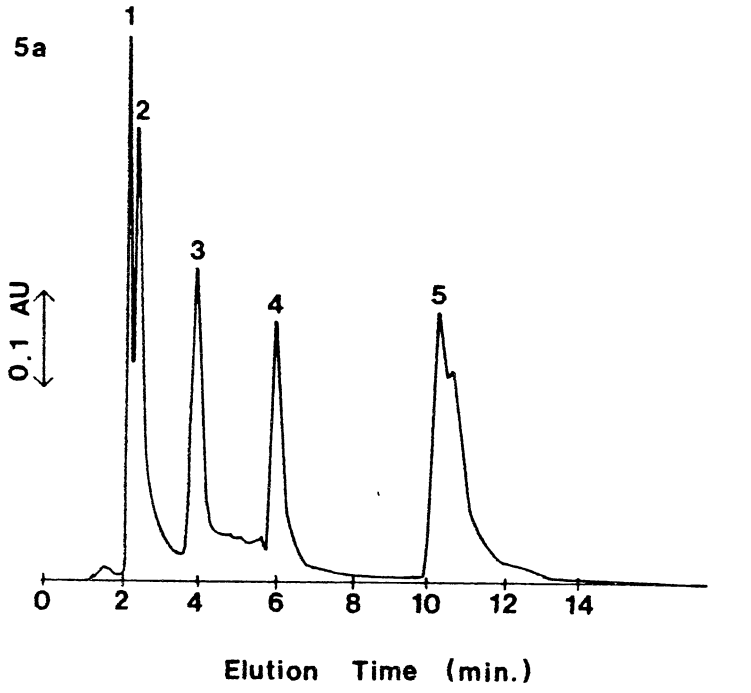
5a
1
2
3
4
5
0.1 AU
0
2
4
6
8
10
12
14
Elution Time (min.)

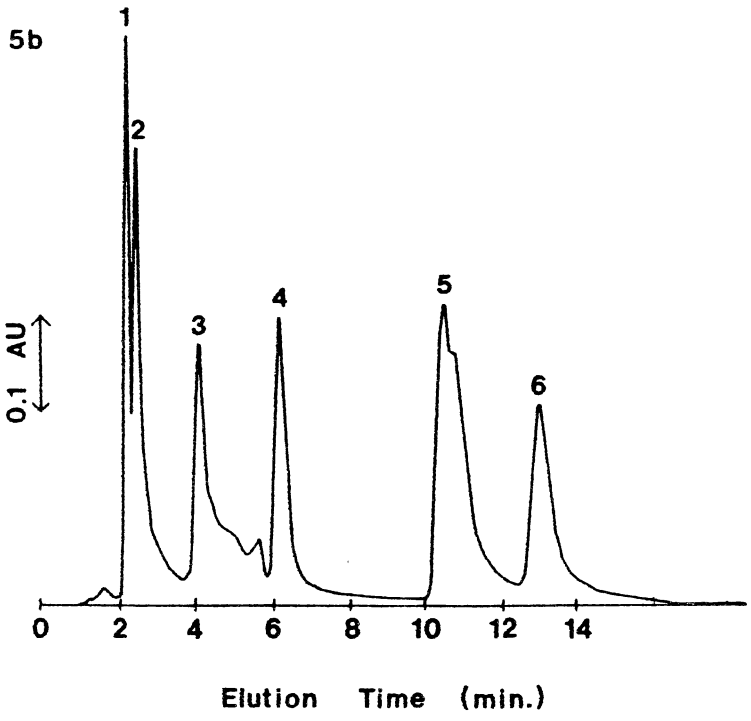
5b
1
2
3
4
5
6
0.1 AU
0
2
4
6
8
10
12
14
Elution Time (min.)

Cyclic Nucleotide Phosphodiesterase Assay

The effect of calmodulin on 3', 5' cyclic nucleotide phosphodiesterase was measured by the formation of ^{3}H-adenosine as described by Wallace et al. (163). Reaction mixtures contained 40 mM Tris-HCl, pH 8.0, 3 mM $MgSO_4$, 50 μM $CaCl_2$, and 0.0033 units of activator-deficient cyclic nucleotide phosphodiesterase. Calmodulin was diluted with 0.1% lipid-free BSA and sufficent H_2O was added to make a total volume of 0.08 ml. The reactions were initiated by the addition of 20 μl of 10 mM ^{3}H-cAMP (specific activity 6.75 μCi/mmol) and incubated at 30°C for 30 minutes. The reactions were terminated by heating in an boiling water bath for 1 minute. The reactions mixtures were re-equilibrated to 30°C and 20 μl of a 1 mg/ml solution of Crotalus atrox venom was added and the mixtures were incubated for an additional 10 minutes. In order to remove ^{3}H-cAMP and ^{3}H-AMP from the reaction mixtures, 1 ml of a 33% (v/v) slurry of Dowex 1x2 was added and the tubes were gently vortexed. The tubes were then centrifuged for 10 minutes in a clinical centrifuge to sediment the resin. Determination of ^{3}H-adenosine was carried out by counting a 0.5 ml aliquot of the supernatant with 10 ml of Insta-Gel using a liquid scintillation counter. The samples were counted for 5 minutes each and the counts per minute were converted to disintegrations per minute by the external sample channels ratio method with a set of Beckman quenched ^{3}H standards. The net dpm for each reaction was calculated after correcting for residual ^{3}H-cAMP in the supernatant and the recovery of adenosine. The efficiency of cAMP binding to the Dowex resin was 95-97% and the recovery of adenosine was 51%.

For studies on the effect of trifluoperazine on calmodulin activation of cyclic nucleotide phosphodiesterase, the same method was used as described above except 0.27 pg of calmodulin was added to activate the enzyme. Appropriate dilutions of trifluoperazine were then added to the reaction mixtures prior to the addition of ^{3}H-cAMP.

Optimum Calcium Phosphate:Protein Ratio Determination

The adsorption of NAD^+ kinase to calcium phosphate gel was dependent on the amount of gel added to the enzyme solution. Since the binding affinity of the gel may vary with age, percentage of water in the slurry, and from preparation to preparation, the optimum calcium phosphate to protein ratio was determined prior to use of this gel. In order to determine this ratio, various amounts of the calcium phosphate slurry (0 to 1.25 ml) are placed into 15 ml glass centrifuge tubes. Approximately 1 ml of heat treated NAD^+ kinase solution is added to each tube and the tubes are allowed to sit on ice for 15 minutes with occasional mixing. The tubes are then centrifuged at 2445 x g for 10 minutes. The supernatant above each pellet is removed and measured in a 10 ml graduated cylinder. A 100 µl aliquot from each of the supernatants is removed for assay with the standard NAD^+ kinase assay using a 30 minute incubation time. The total residual NAD^+ kinase activity remaining in each of the supernatants is calculated and plotted against the amount of calcium phosphate gel added. From this graph, the optimum amount of calcium phosphate gel per ml of enzyme solution to bind the majority of NAD^+ kinase activity can be determined. Typically, 0.5 to 0.75 ml of calcium phosphate slurry per ml of enzyme solution were required to bind NAD^+ kinase.

Magnesium Calculations for Product Inhibition Studies

For product inhibition studies with $Mg^{++}ADP$, the desired amounts of additional Mg^{++} to add to ADP stock solutions were calculated using the appropriate disassociation constant. A free Mg^{++} concentration of 5 mM was used throughout the studies. The $Mg^{++}ATP$ substrate consisted of equimolar amounts of Mg^{++} and ATP. In order to determine the amount of Mg^{++} to add to ADP, the following equation from (164) was used:

$$M_{add} = \frac{M_f \times [ADP]}{K'd + M_f}$$

where M_{add} denotes additional Mg^{++}, M_f denotes free Mg^{++}, and K'd represents the apparent disaasociation constant of the $Mg^{++}ADP$ complex. K'd for $Mg^{++}ADP$ is equal to 1/k' where k' is the apparent association constant which is dependent on pH and alkali metal concentration. The value of this constant at pH 8.0 can be calculated by the general formula:

$$k'Mg^{++}ADP = kMg^{++}ADP / 1 + 6 \times [AM]$$

where $kMg^{++}ADP = 2.51 \times 103\ M^{-1}$ and the alkali metal concentration ([AM]) for N-ethylmorpholine buffers can be calculated by the following equation:

$$[AM] = 3 \times [ADP] + 4 \times [ATP]$$

After calculating the appropriate amount of Mg^{++} to add at each ADP concentration, stock solutions were prepared and adjusted to pH 8.0.

Preparation of DEAE-Biogel A

DEAE-Biogel A was supplied in the preswollen form from Bio-Rad Laboratories. The gel was degassed for 30 minutes and packed onto a 1.7 x 40 cm glass column which had been silanized to reduce wall effects. The column was equilibrated with 0.01 M potassium phosphate, pH 7.5 at 4°C. Good flow rates were obtained at 0.3 to 0.5 ml/min. Regeneration of the gel to remove absorbed biological materials can be accomplished by washing the column with 1 bed volume of 0.5 N NaOH, followed by a wash with an excess of starting buffer until the pH of the eluent returned to pH 7.5.

Preparation of Sephadex G-150

G-150-120 was hydrated by dissolving 20-25 gms of the fine powder in 1 l of water. The gel could be completely hydrated by allowing it to stand for 3 days at room temperature or by heating the gel at 90°C in a water bath for 5 hours. Both procedures are outlined in a technical brochure available from Pharmacia (165). After swelling, the gel was degassed, if necessary, and equilibrated at 4°C for several hours. The gel slurry was

packed into a silanized 2.6 x 90 cm glass column at 4°C while maintaining a head pressure of 15 cm. Packing the column required 4 to 6 hours. In order to prevent nonspecific binding of biological material to the gel matrix, 2 ml of a solution containing 100 mg of BSA and 0.4 gms of sucrose was applied to the column and allowed to elute through. The separation characteristics of the column were determined by applying and eluting a set of standards consisting of: Blue dextran, BSA, ovalbumin, a-chymotrypsinogen, cytochrome c, and DNP-alanine. The column could be stored for long periods of time with 0.02 % sodium azide.

Preparation of Affinity Gels

Blue Sepharose, 5'AMP-Sepharose, ATP-agarose, and NAD^+-agarose were supplied in a dehydrated form and were swollen in an excess of water. Reactive Red 2 -agarose was supplied in a preswollen form. The gels were washed several times with water to remove any unbound ligand. The gels were then washed with 1 M glycine, pH 8.9 for 1 hour in ordered to block any unreacted sites on the resin and reduce nonspecific binding. The gels were again washed with an excess of water and then packed into 0.5 x 10 cm glass columns. The columns were then equilibrated with 5 mM l-cysteine, 0.05 M Tris-HCl, pH 8.0 at 4°C and were ready for use.

Disc Gel Electrophoresis

The disc gel electrophoretic procedures as described by David (166) were used for analyzing the purity of NAD^+ kinase preparations. Typically, a 50 µl aliquot of Blue Sepharose treated enzyme containing 26-30 µg of protein was mixed with 12.5 µl of 0.005 bromophenol blue in 50% glycerol, 12.5 µl of stacking buffer, pH 6.8, and 50 µl of 40% sucrose. The sample was then applied to tube gels consisting of a 7.5% separating gel with a pH of 8.9 and a stacking gel of pH 6.8. Samples were run at room temperature at a constant current of 1 mA per tube until the sample had reached the top of the separating gel

and then the current was increased to 2 mA per tube. Running time for the gels was about 4 hours. The inside diameter of the gel tubes was 4 cm with a 9 cm long separating gel and a 1.5 cm stacking gel . Gel scans were run on an Auto-Scanner from Helena Laboratories.

Other Methods

Scintillation counting was done on a Beckman Liquid Scintillation Spectrometer Model LS-3150T. Quench correction by the external standard channels ratio and determination of counting effiency were carried out using Packard quenched standards for ^{14}C or a set of Beckman quenched standards for ^{3}H. Counting efficiencies for ^{14}C and ^{3}H were 87-92% and 30 to 31%, respectively.

Protein monitoring and enzyme assays were made in a Hitachi Model 100-80 Spectrophotometer. Protein determinations were made with the Bio-Rad protein assay method (available commercially from Bio-Rad). Standard curves were prepared from 10 mg/ml solutions of bovine serum albumin. Absorbance was determined with the Hitachi spectrophotometer.

Conductivity of the fractions eluted with the gradient in the DEAE-Biogel A step was measured with a Radiometer Conductivity Meter, Type CDM 2d.

The concentration of Mg^{++} ion in a 1 M $MgCl_2$ stock solution was determined by atomic absorption spectrometry which was kindly performed by the Water Quality Laboratories at Oklahoma State University.

Concentration methods utilized an Amicon ultrafiltration cell Model 52. PM-30 ultrafiltration membranes were used with this apparatus.

Computer analysis of the kinetic data obtained in the initial velocity and product inhibition studies was carried out using the programs described by Cleland (167). The programs used had been adapted for use with a CP/M operating system on an Apple microcomputer. These programs were kindly furnished by Dr. R. C. Essenberg, Department of Biochemistry, Oklahoma State University.

Chemicals

The U-^{14}C-NAD$^+$ and ^{3}H-cAMP utilized in these studies were purchased from Amersham. Hydroxymercuribenzoate, N-ethylmaleimide, isocitrate, isocitrate dehydrogenase, the adenine nucleotides, GTP, TTP, CTP, ITP, tripolyphosphate, tetrapolyphosphate, Tris, ammonium phosphate, the pyridine nucleotides, bovine serum albumin, N-ethylmorpholine, dithiothreitol, l-cysteine, and cAMP were purchase from Sigma Chemical Company. DTNB and $MgCl_2$, gold label, were obtained from Aldrich Chemicals. Acetonitrile and methanol were purchased from J.T. Baker Chemical Company. All other chemicals were obtained from major supply houses.

Chromatography Materials

Dowex 1x2 chloride form, 200-400 mesh; Sephacryl S-300, and Sephadex G-150 were purchased from the Sigma Chemical Company. Also, Sigma was the source of Blue Sepharose, Reactive Red 2-Agarose, 5' AMP-Sepharose, and NAD$^+$-Agarose. DEAE-Biogel A was purchased from Bio-Rad Laboratories. A LiChrosorb RP-18 HPLC column was purchased from Curtin Matheson Scientific, Inc. Calcium phosphate gel was the generous gift of Dr. C. A. Yu.

CHAPTER IV

RESULTS AND DISCUSSION

Purification of NAD^+ Kinase

Preparation of Crude Homogenate and Salt Fractionation

Livers were excised from 24 Fischer-344 rats. The rats were sacrificed by decapitation and bled. The excised livers were placed in a chilled beaker containing ice-cold 0.05 M Tris-HCl, pH 7.5. The livers were then rinsed extensively with the buffer to remove any fat, hair, and other debris. The livers were trimmed of any noticeable connective tissue and weighed. Approximately 258.7 g of liver were obtained. The livers were minced with scissors and the excess buffer was decanted. The liver mince was homogenized in 200 ml of buffer with a tight-fitting glass mortar equipped with a teflon pestle. After homogenization, buffer was added to bring the total amount of buffer to approximately 4 times the liver weight. The total volume of the crude homogenate was 1318 ml. The crude homogenate was centrifuged for 1 hour at 36,600 x g. The pellet was discarded and 1020 ml of the supernatant was ready for further purification.

In all purification steps, a 1.5 to 2 ml aliquot was removed for assay and protein determination. The standard assay for NAD^+ kinase was used for all activity determinations.

The next step in the purification procedure was salt fractionation by the addition of ammonium sulfate to the crude homogenate supernatant. The solution was brought to 30% saturation in ammonium sulfate by the addition of 165.9 g of finely ground ammonium sulfate to the 1018 ml of the supernatant, which was stirring at 4°C. After completion of

this addition, the mixture was allowed to stand on ice for 30 minutes and then centrifuged for 30 minutes at 36,600 x g. The pellets were discarded and the supernatant was further fractionated by the addition of 193.4 g of ammonium sulfate to bring the final concentration to 57% saturation. During the additions of ammonium sulfate, the pH of the mixture was maintained above pH 7.2 by the dropwise addition of 1.0 N NaOH. After completion of the second addition, the mixture was allowed to stand on ice for 30 minutes and then centrifuged at 36,600 x g. The supernantant was discarded and the protein pellets were resuspended with 250 ml of 0.05 M Tris-HCl, pH 8.0. The suspension was placed in standard dialysis tubing and dialyzed against 8 L of 0.05 M Tris-HCl, pH 8.0 at 4°C for 12 hours. The dialysates were combined for a total volume of 306 ml. A 3 ml aliquot was removed for assay and protein determination.

Ammonium sulfate fractionation of the crude homogenate supernatant solution resulted in a 2-fold increase in the yield of the enzyme based on the assays at each step. This increase in the yield after ammonium sulfate fractionation was also noted in subsequent preparations. Initially, it was thought that the increase could be due to the removal of a component inhibitory for NAD^+ kinase, present in the crude homogenate, during salt fractionation. Assay of a dialyzed sample of the supernatant obtained after the 57% ammonium sulfate cut with NAD^+ kinase resulted in an inhibition of $NADP^+$ formation (168). However, further investigation into this phenomenon showed that the observed inhibition could be due to the presence of a component in the crude homogenate which may interfere with determination of NAD^+ kinase by the spectrophotometric assay (R. K. Gholson, unpublished observations). The exact nature of this effect, however, remains to be established.

Heat Treatment

The remaining 303 mls. of the dialyzed enzyme solution was divided equally into two 250 ml Erlenmeyer flasks equipped with 1-hole stoppers and thermometers. The flasks

were then incubated in a 60°C water bath. The temperature of the enzyme solutions inside the flasks was allowed to reach 60°C and maintained at that temperature for 5 minutes. The flasks were removed from the water bath and cooled on ice for 1.5 hours. The temperature of the enzyme solutions after this period was less than 5°C. The enzyme solution was then centrifuged for 30 minutes at 41,500 x g to sediment coagulated protein. An extra 25 ml of 0.05 M Tris-HCl, pH 8.0, was used to rinse any residual enzyme solution from the flasks just prior to centrifugation. The pellets were discarded and the supernatant was used for further purification. The total volume of the supernatant was 246 ml. A 1.5 ml aliquot was removed for assay and protein determination and an additional 7 ml were removed for determining the optimal calcium phosphate gel: protein ratio.

The recovery at the heat treatment step was typically 85% of the previous steps activity. This step also resulted in a four-fold reduction in the total protein. The 41,500 x g centrifugation was necessary to insure that all the coagulated protein was sedimented.

Optimum Calcium Phosphate:Protein Ratio

The 7 ml aliquot removed from the heat-treated enzyme was used to determine the optimum calcium phosphate:protein ratio. This procedure is described in the "Materials and Methods" section. A plot of residual NAD^+ kinase activity as a function of added calcium phosphate can be seen in Figure 6. Based on the graph, it was judged that 0.65 ml of calcium phosphate slurry was to be added per ml of enzyme solution to absorb most of the NAD^+ kinase activity from the heat-treated solution.

Calcium Phosphate Extraction

A rough separation based on charge was carried out using calcium phosphate. Based on the previous determination of the optimal calcium phosphate gel:protein ratio, approximately 150 ml of calcium phophate gel slurry (227 mg/ml - dry weight) was added to 235 ml of heat-treated enzyme. The mixture was allowed to stir at 4°C for 30 minutes

Figure 6. A Plot of Residual NAD^+ Kinase Activity Versus Added Calcium Phosphate. See text for experimental details.

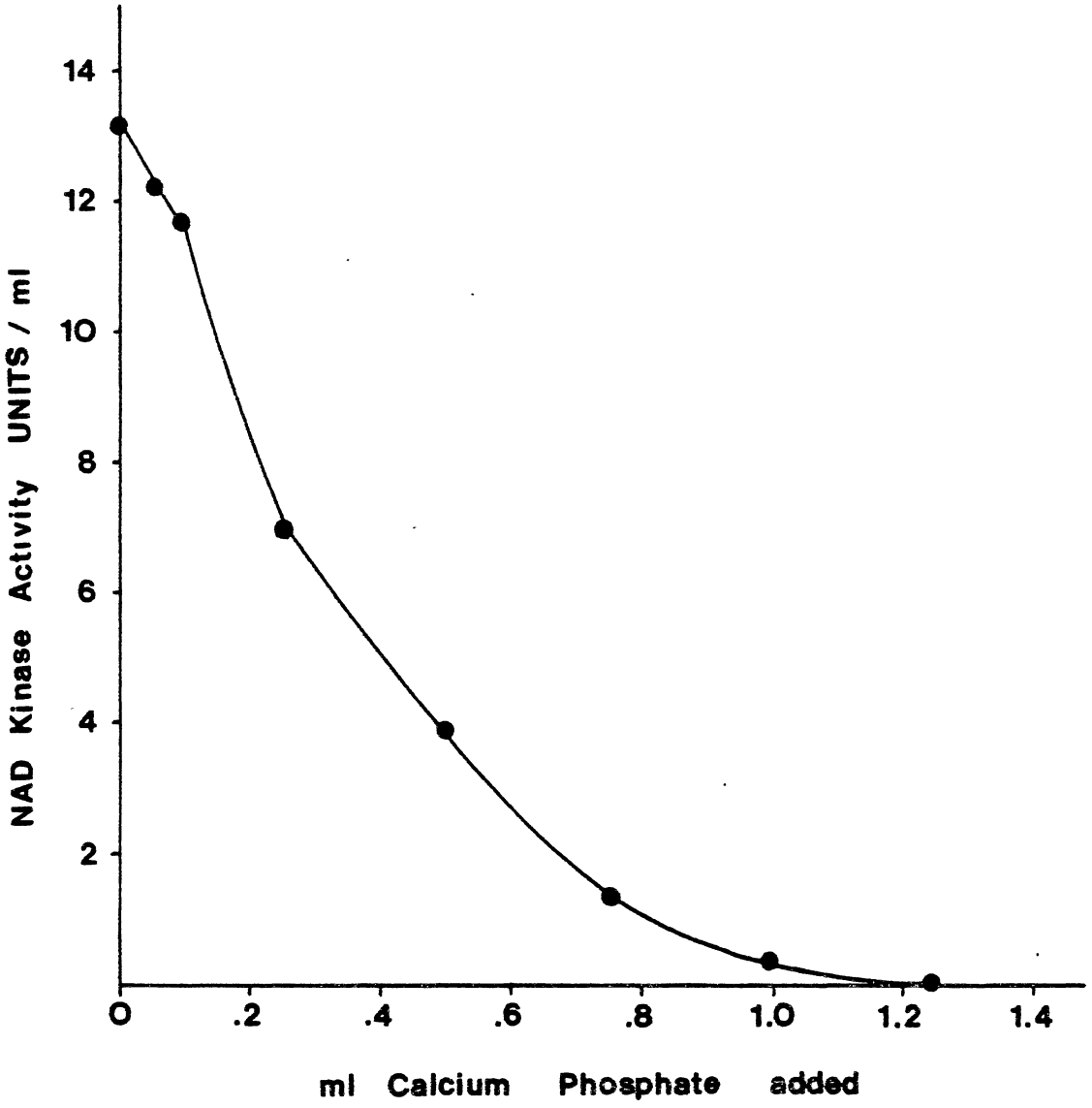
NAD Kinase Activity UNITS / ml
14
12
10
8
6
4
2
0
.2
.4
.6
.8
1.0
1.2
1.4
ml Calcium Phosphate added

and then was centifuged for 10 minutes at 2445 x g. The supernatant was discarded and the calcium phosphate pellet was washed by resuspending the pellet in 200 ml of 0.05 M Tris-HCl, pH 8.0 for 15 minutes. The suspension was then centrifuged for 10 minutes at 2445 x g. The supernatant was discarded and the pellet was washed a second time using the same procedure.

Following the second wash, the calcium phosphate pellet was extracted by resuspension in 80 ml of 0.5 M potassium phosphate, pH 7.5 for 25 minutes at 4°C. The mixture was then centrifuged for 10 minutes at 2445 x g. The supernantant was decanted and saved. The pellet was re-extracted with 75 ml of the potassium phosphate buffer for 25 minutes at 4°C. The mixture was again centrifuged for 25 minutes at 2445 x g. The supernatant was decanted and the calcium phosphate pellet was discarded. The supernatants from the two extractions were combined and centrifuged for 10 minutes at 8500 x g. This centrifugation was necessary to remove the fine particles of calcium phosphate gel which decanted with the supernatants. The small pellets were discarded and the supernatants were placed into standard dialysis tubing and dialyzed for 12 hours against 8 L of 0.01 M potassium phosphate, pH 7.5. The dialysates were combined for a total volume of 166 ml. A 3 ml aliquot was removed and the remaining dialysate was divided into two equal portions. One portion was frozen at -20°C and the second portion was used immediately for further purification.

The recovery of the enzyme after the calcium phosphate step was generally 65 to 75% of the previous step's activity. In later preparations, monitoring the residual enzyme activity in the supernatant after calcium phosphate addition indicated that virtually all the activity was bound to the gel. This suggests that the recovery of NAD^+ kinase at this step might be increased by using a higher ionic strength extraction buffer or by increasing the extraction time with the 0.5 M potassium phosphate buffer.

DEAE-Biogel A Chromatography

A second separation based on charge was carried out using DEAE-Biogel A. A 1.7 cm x 35 cm column of DEAE-Biogel A was packed and equilibrated at 4°C with 0.01 potassium phosphate, pH 7.5. A portion of the calcium phosphate extracted enzyme (83 ml) was applied to the top of the column using a resevoir. After the enzyme had been absorbed the column was washed with 330 ml of the equilibration buffer. After this wash, the absorbance of the effluent at 280 nm had dropped below 0.05 absorbance unit. This wash was discarded and the column was eluted with a linear gradient from 0.01 to 0.4 M potassium phosphate, pH 7.5 (160 ml each) and 3 ml. fractions were collected. The column could be run in a total time of 16 to 20 hours. In order to select the proper fractions with NAD^+ kinase activity to be pooled, 100 µl of the gradient fractions were assayed and fractions with an activity greater than 0.573 units/ml were pooled. Fractions 53 to 82 were combined, making the total pooled eluent volume 76 ml. An activity and protein profile can be seen in Figure 7. The peak of NAD^+ kinase activity typically followed the first protein peak eluted with the gradient.

A second DEAE-Biogel A column was run with the remainder of the calcium phosphate-treated enzyme. The frozen calcium phosphate fractionated enzyme (76 ml) was thawed at 4°C for 12 hours and then applied to the top of a second DEAE-Biogel A column via a reservoir. The column wash, linear gradient elution, and the locating of NAD^+ kinase activity in the gradient fractions were performed as described above. With the second column, gradient fractions 51 through 83 were then combined, making the total volume of the pooled eluent 82 ml. A 2 ml aliquot was removed for assay and protein determination. The pooled DEAE-eluents from both columns were maintained at 4°C to await further purification.

The recovery of the DEAE-Biogel A step was typically 70% of the previous steps activity. This was primarily due to protein denaturation while on the column and through a small amount of the enzyme being lost in the column wash with 0.01 M potassium

Figure 7. DEAE-Biogel A Chromatography of NAD^+ Kinase.

NAD^+ kinase activity is expressed in units per ml and is represented by the following: ●—●. Protein absorbance was measured at 280 nm and is represented by: ■—■ and the conductivity of the fractions is denoted by ▲—▲. See text for experimental details.

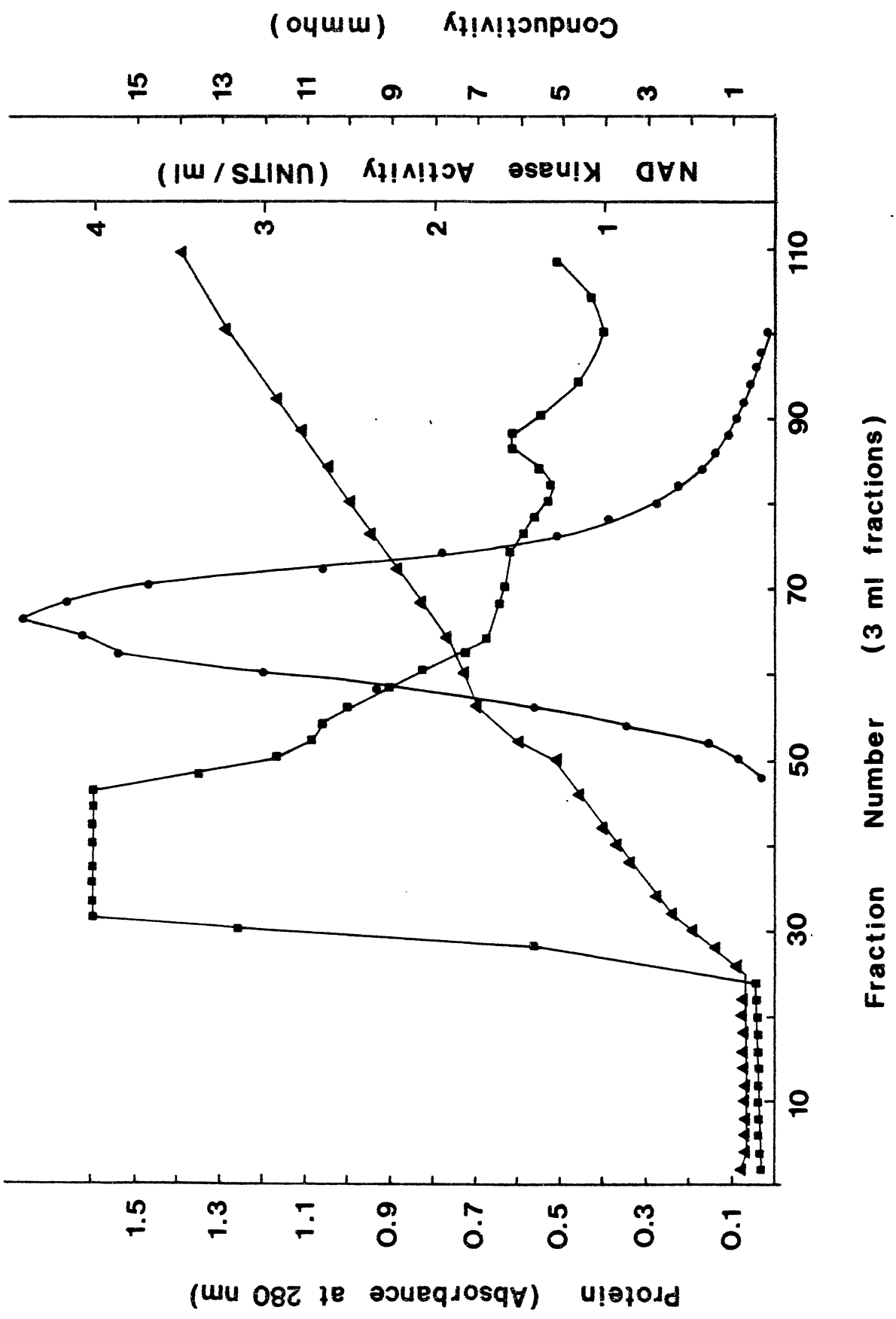
Protein (Absorbance at 280 nm)
0.1
0.3
0.5
0.7
0.9
1.1
1.3
1.5
NAD Kinase Activity (UNITS / ml)
1
2
3
4
Conductivity (mmho)
1
3
5
7
9
11
13
15
10
30
50
70
90
110
Fraction Number (3 ml fractions)

phosphate, pH 7.5. In addition, the activity of the calcium phosphate extract which had been stored for two days at -20°C was generally lower than the extract which was immediately applied to the column. For this reason, the two pooled samples were used separately throughout the final stages of purification.

In order to reduce the volume of the pooled DEAE-Biogel A effluents for application to a Sephadex G-150 column, they were concentrated by precipitation by dropwise addition of 1.3 ml of saturated ammonium sulfate per ml of effluent over a 30 minute period at 4°C. This addition brings the final concentration of ammonium sulfate in the solution to 57%. The pH of the mixture was maintained above pH 7.4 by the dropwise addition of 1.0 N NaOH. Following the final addition of saturated ammonium sulfate, the mixture was allowed to stand at 4°C for 30 minutes and then centrifuged for 30 minutes at 36,600 x g. The supernatant was discarded and the pellet was resuspended in 4 mls of 0.01 M potassium phosphate, pH 7.5.

Sephadex G-150 Gel Filtration

A 2.5 x 85 cm column was packed with swollen G-150-120 at 4°C and equilibrated with 0.01 M potassium phosphate, pH 7.5. The ammonium sulfate concentrate of the DEAE-effluent containing 0.4 g of dissolved sucrose was layered underneath the buffer at the top of the gel bed. The column was eluted at 4°C with the equilibration buffer using a 15-cm head. The column flow rate was about 12 ml per hour and 3 ml fractions were collected. The column was eluted in about 20 hours. The fractions were assayed for activity and fractions containing greater than 0.573 units per ml were pooled. Fractions 44-59 were combined for a total volume of 40 mls. A 3 ml aliquot was removed for assay and protein determination. A protein and activity profile are shown in Figure 8.

The recovery of the G-150 Sephadex step was generally 50 to 60%. Gel filtration was used at this step due to a sufficient reduction of total protein by the DEAE-Biogel A step to avoid overloading the column. A comparison of the elution profile with a group of

Figure 8. Elution Profile of NAD^+ Kinase on Sephadex G-150.

NAD^+ kinase activity is measured in units per and is represented by the following: □—□. Protein absorbance was measured at 280 nm and is denoted by: ■—■. See text for experimental details.

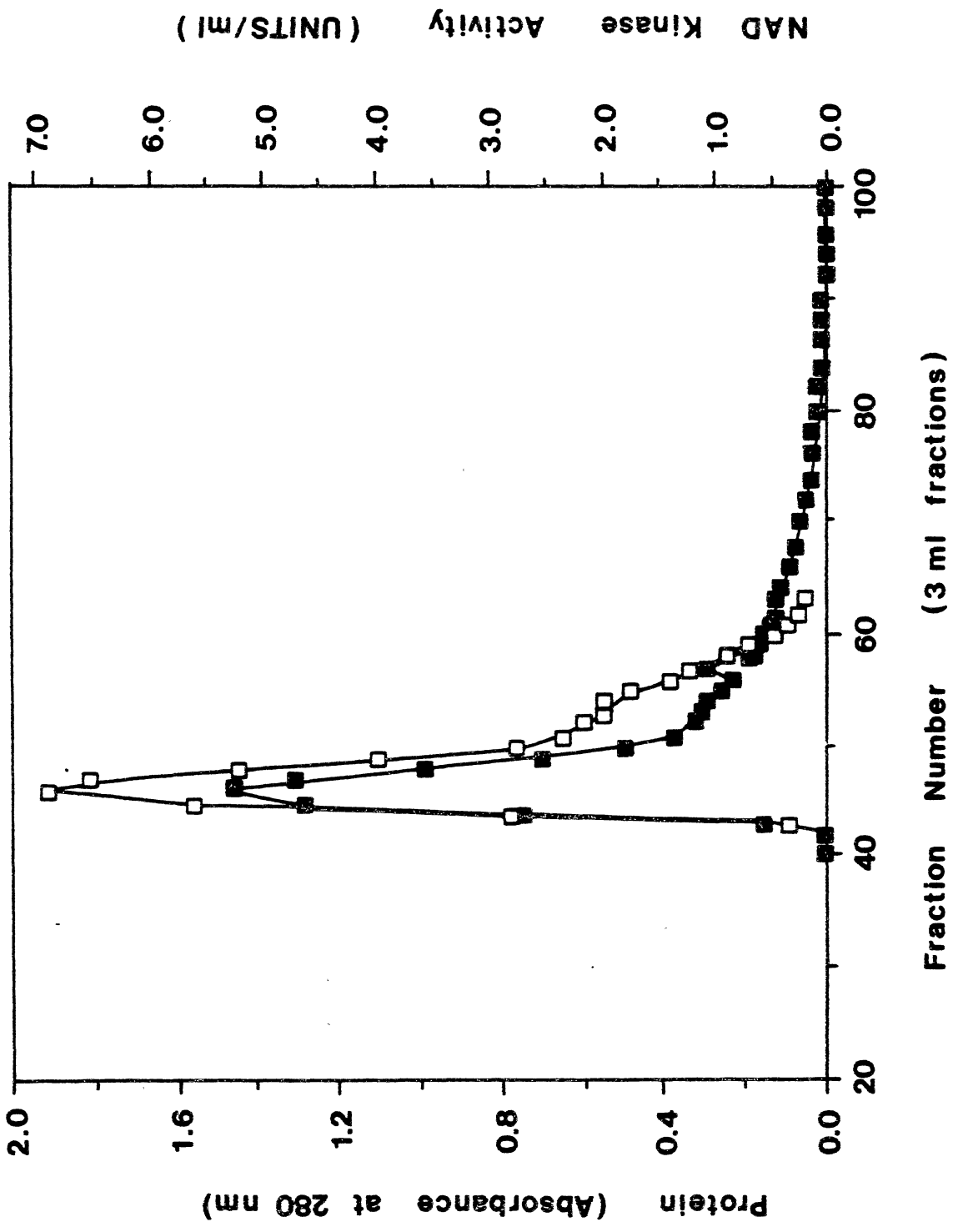
Protein (Absorbance at 280 nm)
2.0
1.6
1.2
0.8
0.4
0.0
NAD Kinase Activity (UNITS/ml)
7.0
6.0
5.0
4.0
3.0
2.0
1.0
0.0
20
40
60
80
100
Fraction Number (3 ml fractions)

standards run prior to sample application, indicated that the peak of NAD^+ kinase activity migrates with the void volume on Sephadex G-150. Although no accurate molecular weight determination is possible, Sepadex G-150 chromatography gave a 1.4-fold increase in purification and was routinely used.

The G-150 effluent was again concentrated for the next purification step by ammonium sulfate precipitation as described previously. The supernatant was discarded and the protein pellets were resuspended in 4 ml of 0.05 M Tris-HCl, pH 8.0 containing 5 mM l-cysteine. The solution was dialyzed at 4°C for 12 hours against 4 L of this buffer. The dialysate was removed from the tubing and had a total volume of 4.8 ml. A 0.5 ml aliquot was removed for assay and the remainder of the dialysate was used in the next purification step.

Blue Sepharose Affinity Chromatography

The final step used in purification of NAD^+ kinase was affinity chromatography on Blue Sepharose. Cibracon blue F3G-A, the chromatophore in Blue Sepharose, belongs to a family of triazine dyes which have been shown to bind to dehydrogenases and kinases. Although the true basis of the protein-dye interactions is unclear, the chromatophore appears to be specific for a nucleotide binding site called the dinucleotide fold. Cibracon blue F3G-A has been shown to bind tightly to pigeon liver NAD^+ kinase (169). Complete removal of the dye from the enzyme could not be achieved by dialysis, gel filtration, or charcoal adsorption. Blue Sepharose, however, has been successfully employed in the purification of NAD^+ kinase from C. utilis (89).

A 0.5 x 8 cm column of hydrated Blue Sepharose was packed and equilibrated at 4°C with 0.05 M Tris-HCl, pH 8.0 containing 10 mM $MgCl_2$. A 3.8 ml sample of the dialyzed concentrate from the G-150 step was applied to the column. Previous determinations of the behavior of NAD^+ kinase on Blue Sepharose showed that an increase in the amount of time that the sample was in contact with the affinity gel increased the amount of activity bound.

Based on this observation, the column was turned off for 1 hour. After this time period, the column was washed with 50 mls. of 0.05 M Tris-HCl, pH 8.0 containing 5 mM l-cysteine. Elution of NAD^+ kinase was accomplished by applying 1.5 M NaCl dissolved in the wash buffer. Fractions of 3 ml. were collected at 4°C over a period of 3 hours. The fractions were then assayed for activity. Using these conditions, the NAD^+ kinase eluted from the column was present in the third fraction obtained after the start of the 1.5 M NaCl elution. The fraction was then dialyzed for 8 hours against 4 L of 0.05 M Tris-HCl, pH 8.0 containing 5 mM l-cysteine. The dialysate had a volume of 2.8 ml and a 0.8 ml aliquot was removed for assay, protein determination, and disc-gel electrophoresis. The remainder was then stored at -20°C. Figure 9 is a protein and activity elution profile from the Blue Sepharose step.

Recovery from the Blue Sepharose step was 35% of the activity applied. This may be due, in part, to a portion of the activity which was not bound to the column or had run through the column before the flow was stopped. Although steps were taken in the preparation of the gel to reduce nonspecific binding, this may be a factor in the recovery of NAD^+ kinase. Previous experiments in using biospecific elution of NAD^+ kinase from the column with 20 mM NAD^+ were unsuccessful. It may be possible to use ATP or a structural analog of either NAD^+ or ATP to achieve a biospecific elution and improve the purity of the final preparation of NAD^+ kinase. Alternatively, it may be possible to establish gradient conditions based on an increase in ionic strength to elute NAD^+ kinase from the column. The use of a gradient elution may result in an enhanced purification of the enzyme by avoiding the desorption of other bound materials which may occur at higher ionic strengths.

Evaluation of the Purification of NAD^+ Kinase

The purification procedure provides an enrichment of specific activity of about 2000-fold with an 18% recovery of original activity. The purification summary is presented in

Figure 9. Blue Sepharose Affinity Chromatography of NAD^+ Kinase.

NAD^+ kinase activity is measured in units per ml and is represented by: o---o. Protein absorbance was measured at 280 nm and is denoted by: ●—●. The arrow indicates the beginning of the elution of NAD^+ kinase activity with 1.5 M NaCl dissolved in 5 mM l-cysteine, 0.05 M Tris-HCl, pH 8.0. See text for experimental details.

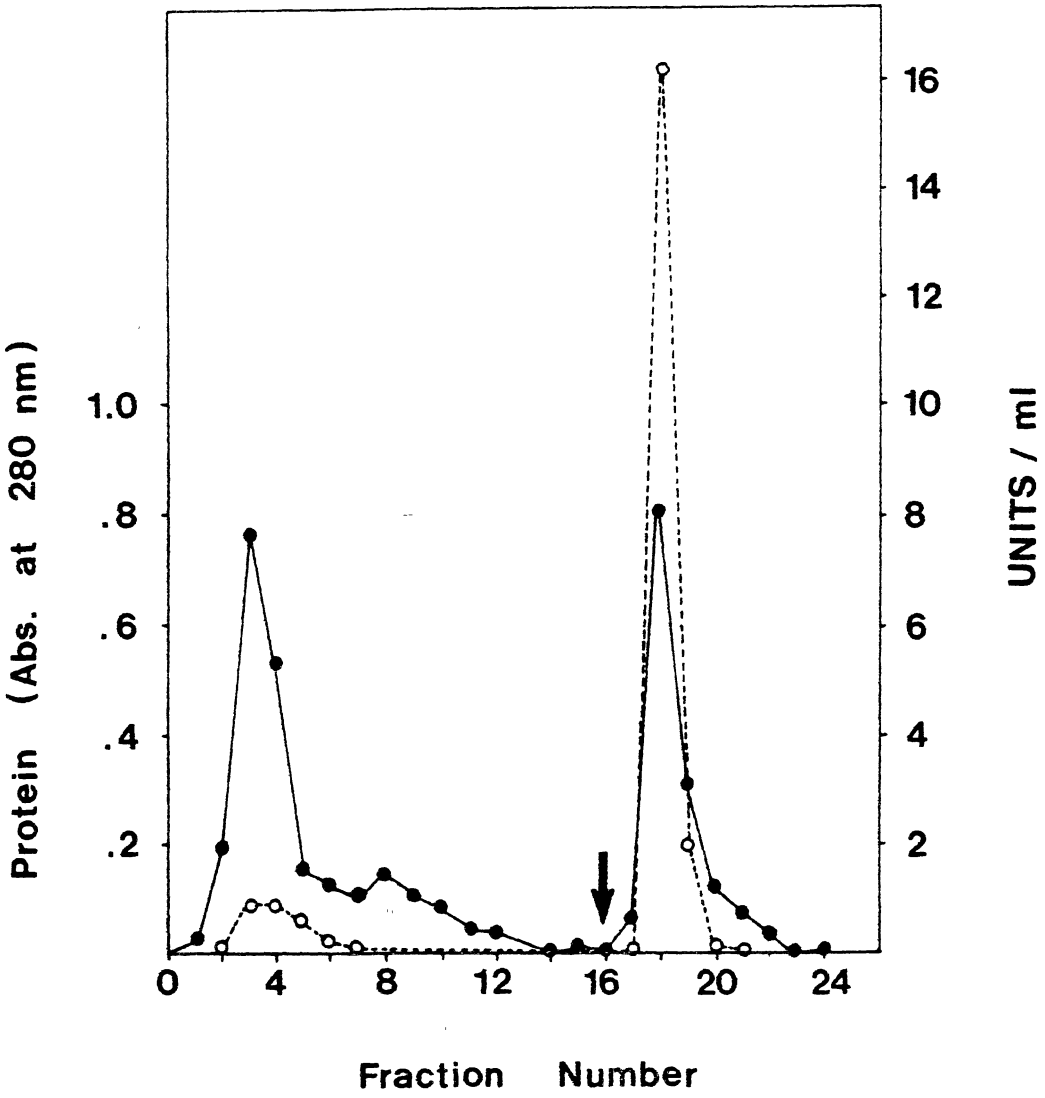
Protein (Abs. at 280 nm)
1.0
.8
.6
.4
.2
0
4
8
12
16
20
24
Fraction Number
16
14
12
10
8
6
4
2
UNITS / ml

Table III. As mentioned previously, the increase in the yield of the enzyme after ammonium sulfate fractionation may be due to the loss of a component which interferes with the determination of NAD^+ kinase activity or inhibits the enzyme. The storage of half of the preparation after the calcium phosphate step for 2 days at -20°C resulted in the loss of some enzymatic activity which affected the specific activity determinations in subsequent steps (see Table IIIb). However, the storage of a portion of the calcium phosphate step made the purification procedure easier and was routinely used.

The problem of denaturation of NAD^+ kinase in dilute solutions was partially prevented by the addition of a stabilizing agent. Yero et al. (92) reported that the inclusion of a mild reducing agent, 5 mM l-cysteine, had a stabilizing effect on NAD^+ kinase. For this reason , l-cysteine was included in the buffers in the final step of purification.

Other Methods

Gel Filtration

Since NAD^+ kinase activity migrates with the void volume on Sephadex G-150, other gels with a greater molecular weight separation range were tried. Chromatography of NAD^+ kinase on Sephadex G-200 was tedious and time-consuming due to the inherently low flow rates encountered with this gel. The gel was also susceptible to slight variations in the head pressure which led to an eventual stoppage of flow through the column. Sephacryl S-300, which consists of acrylamide cross-linked to dextran beads, is less susceptible to changes in the head pressure and has faster flow rates than comparable Sephadex gels. The recovery of NAD^+ kinase activity was negligible after chromatography on this gel. This may be due to the binding of the enzyme to the gel matrix since little activity was detected in the eluent. Sephacryl S-300 might possibly be used for gel filtration of NAD^+ kinase if the right elution conditions can be found to prevent the adsorption of the enzyme to the gel.

TABLE III

PURIFICATION OF NAD^+ KINASE FROM RAT LIVER

		Protein			Enzyme			
		Volume (ml)	Concentration (mg/ml)	Total (mg)	Specific Activity (unit/mg)	Total Activity (units)	Fold Purification	Yield (%)
I. Crude Homogenate		1318.	26.0	34268.	.0114	390	1.00	100.
II. Ammonium Sulfate Fractionation: 30-55%		306.	30.4	9302.	.0875	816	7.7	210.
III. Heat Extraction		236.	7.4	1746.	.399	697	35.	178.
IV. Calcium Phosphate Adsorption		166.	4.5	747.	.692	517	61.	133.
V. DEAE-Biogel A Chromatography:	a)	76.	.59	44.8	4.01	176	352.	89.5
	b)	82.	.57	46.7	3.71	173	325.	
VI. G-150-120 Gel Filtration:	a)	40.	.59	21.6	5.67	123	497.	51.2
	b)	34.	.47	16.0	4.84	77	425.	
VII. Blue Sepharose Chromatography:	a)	2.8	.52	1.46	27.9	41	2450.	18.3
	b)	2.6	.54	1.40	22.0	31	1930.	

a) and b) represent two separate runs through the purification scheme.
Run a) was performed with 83 ml of calcium phosphate extracted enzyme.
Run b) was performed with 76 ml of calcium phosphate extracted enzyme

Affinity Chromatography

Although Blue Sepharose was adopted for use in the purification of NAD^+ kinase, several other types of affinity gels were tried in attempts to purify the enzyme under the same application and elution conditions. Reactive Red 120-agarose is available commercially from the Sigma Chemical Company. The triazine dye ligand of this gel is Procion Red HE-3B, which is reported to be more selective for $NADP^+$-requiring enzymes than Cibracon blue F3G-A (170, 171). NAD^+ kinase did bind to the Reactive Red column; however, the enzyme could not be eluted with high ionic strength buffers. ATP-agarose, 5'-AMP-Sepharose, and NAD^+-agarose were also tried. NAD^+ kinase apparently did not bind to these gels, since most of the activity appeared in the equilibration buffer wash. This may be due, in part, to steric hindrances caused by the sidearm or the gel itself which may limit the access of the coenzyme ligand to the enzyme molecule for binding. All possible binding conditions for NAD^+ kinase to these affinity gels were not explored; however, and it may be possible to use these gels in the purification of NAD^+ kinase if the proper adsortion and elution conditions can be found.

Concentration

The purification scheme requires the concentration of the pooled fractions after the DEAE-Biogel A step and after gel filtration on Sephadex G-150. Precipitation of the enzyme activity at 57% saturation with saturated ammonium sulfate generally worked well with almost 100% recovery. An alternative method of ultrafiltration for concentrating the activity was used on later preparations of the enzyme. A PM-30 ultrafiltration membrane (exclusion limit-30,000 daltons) was used at 4°C with 20 pounds per square inch in pressure supplied by a cylinder of nitrogen. Recovery of the activity was complete and this method could concentrate 47 ml of enzyme solution to 2.5 ml in about 2 hours.

Disc Gel Electrophoresis

Analytical polyacrylamide gel electrophoresis was utilized to determine the homogeneity of the Blue Sepharose treated enzyme. Sample volumes of 50 µl containing 25 to 30 µg of protein were used. Disc gel electrophoresis at pH 8.9 in 7.5% separating gels revealed the presence of a single major protein band with an Rf value of 0.16. Doubling the amount of protein applied to the gel increased the intensity of the major protein band and a faint smear became visible at the top of the gel. A photograph of the gel appears in Figure 10. Analysis of the gel on a gel scanner revealed the major band of protein constituted about 60% of the total protein on the gel. A tracing of the gel scan is seen in Figure 10b. Although a single peak corresponding to the major protein band was seen, there may be a sufficient amount of other material present to affect the overall purity of the enzyme. This finding suggests that another purification step may be necessary for the final purification of NAD^+ kinase. Another alternative procedure may be to narrow the number of fractions pooled after the DEAE-Biogel A step and again after the Sephadex G-150 step. This procedure would decrease the overall yield of the enzyme, but may increase the purity in the final step. As mentioned previously, the application of a gradient elution to the Blue Sepharose step may also enhance the purity of the enzyme.

Other samples of purified NAD^+ kinase preparations analyzed by disc gel electrophoresis, also revealed the presence of two smaller bands of protein in addition to the major band of protein. These two bands had R_f values of 0.218 and 0.29, respectively. These two bands may be additional contaminants in the preparations or artifacts produced during electrophoresis. Nemchiskaya et al. (94) have suggested that rat liver NAD^+ kinase may exist in multiple forms. Although there is some uncertainty as to whether or not all the bands seen in their electrophoretic patterns represent different forms of the enzyme, the existence of multiple forms may be an important consideration in judging the final purity of NAD^+ kinase preparations.

Figure 10. Disc Gel Electrophoresis of NAD^+ Kinase.

Disc gel electrophoresis was performed on the NAD^+ kinase sample from the Blue Sepharose step. Figure 10a is a photograph of the gel showing a single major band of protein with an R_f value of 0.16. Figure 10b is a gel scan of the gel.

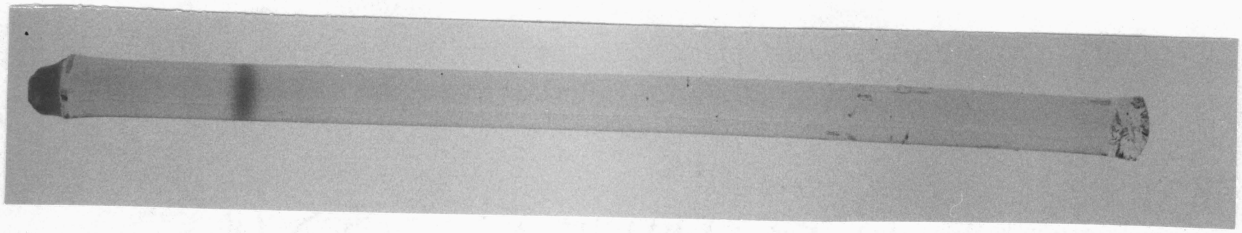

10a

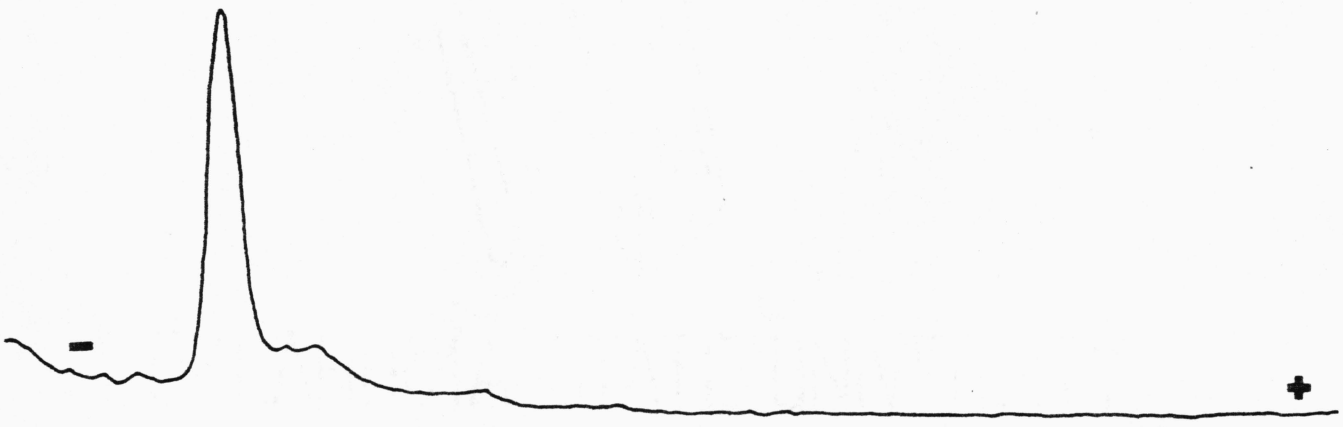

10b

Characterization of NAD^+ Kinase

Nucleoside Triphosphate Specificity

Several different nucleoside triphosphates were sustituted for ATP to test their effects on the velocity of the reaction. Reaction mixtures contained 8 mM NAD^+, 15 mM $MgCl_2$, 200 mM N-ethylmorpholine, pH 8.0, and 10 mM of the appropriate nucleotide in a final volume of 0.45 ml. The reaction was initiated by the addition of 50 µl of NAD^+ kinase and incubated at 37°C. Duplicate reactions were run for 10 min. and 20 min. for each nucleotide used. The reactions were terminated by heat for 1 min. in a boiling water bath and $NADP^+$ formation was determined by the standard spectrophotometric assay. The results from these experiments are presented in Table IV.

Deoxyadenosine triphosphate (dATP) was a slightly more effective phosphate donor in the reaction than ATP. None of the other nucleotides tested were as effective as dATP or ATP. CTP was only partially effective as a substrate for $NADP^+$ formation. The straight chain polyphosphates, tripolyphosphate and tetrapolyphosphate, were not effective phosphate donors. The addition of 10 mM adenosine to the polyphosphate reaction mixtures did not stimulate $NADP^+$ synthesis. NAD^+ kinase seems to have a narrow specificity for the nucleotide phosphate participating in the phosphorylation reaction. The higher velocities attained with dATP as a substrate rather than ATP has also been noted in the NAD^+ kinase from chicken liver (172).

Divalent Cation Specificity

Several different divalent cations were used to replace Mg^{++} to determine their effects on the activation of NAD^+ kinase. Reaction mixtures contained 8 mM NAD^+, 150 mM N-ethylmorpholine, pH 8.0, 10 mM ATP and 15 mM of the appropriate cation. The ATP substrate used came from a stock solution which had been adjusted to pH 8.0. This was done in order to prevent possible pH fluctuations in the reaction mixtures due to the high

TABLE IV

NUCLEOTIDE SPECIFICITY OF NAD+ KINASE[a]

Nucleotide	Units	% Activity[b]
ATP	0.4761	100
dATP	0.5382	113
GTP	0.035	7
TTP	0.033	7
CTP	0.1185	25
ITP	0.02	4
ADP	0	0
AMP	0	0
Tripolyphosphate	0	0
Tetrapolyphosphate	0	0
Tripolyphosphate + Adenosine	0	0
Tetrapolyphosphate + Adenosine	0	0

[a]See text for Experimental Details.
[b]Based on 100% activity with ATP.

levels of ATP used. Mg^{++}, Mn^{++}, Co^{++}, Ca^{++}, Ba^{++}, Cu^{++}, Sn^{++}, and Fe^{++} were added as their chlorides and Zn^{++} was added as its acetate. Duplicate reaction mixtures were run for 10 and 20 minutes for each cation. The reaction was terminated by heating in a boiling water bath and $NADP^+$ produced was detected by the standard spectrophotometric assay. The buffer used in the spectrophotometric assay was 0.05 M Tris-HCl, pH 8.0 containing 10 mM $MgCl_2$. The presence of Mg^{++} ions in this buffer was necessary to fulfill the metal requirements of isocitrate dehydrogenase. As seen in Table V, Mg^{++} was the most potent activator of NAD^+ kinase at the concentration used . The order of effectiveness was $Mg^{++} > Mn^{++} > Co^{++} > Ca^{++} > Cu^{++} > Zn^{++}$. Ba^{++}, Fe^{++}, and Sn^{++} showed no activation. These results are not in complete agreement with those of Yero et al. (92) who proposed that the order of effectiveness was $Mg^{++} > Mn^{++} > Zn^{++} > Fe^{++} > Ca^{++} > Co^{++}$ with rat liver NAD^+ kinase. However, some of the differences in the two results may be due to differences in the experimental conditions used such as buffering systems and metal ion concentrations.

Figure 11 shows the dependence of NAD^+ kinase activity on Mg^{++} concentration. The assays were conducted as previously described for the cation replacement experiment with the exception that Mg^{++} was varied from 0 to 40 mM final concentration. The optimal Mg^{++}:ATP ratio was 1.5 to 1.

The results of cation replacement experiments, such as those presented in Table V and those of Yero and co-workers (92) can be somewhat misleading, since the concentrations of cations used in these experiments may be higher than the optimal concentrations. Therefore, four cations, Mg^{++}, Mn^{++}, Co^{++}, and Zn^{++} were examined to determine the effects of these cations at various concentrations on NAD^+ kinase activity. As can be seen in Figure 12, Mn^{++} was a more potent activator of NAD^+ kinase than Mg^{++} at lower metal concentrations. Zn^{++} also stimulated NAD^+ kinase, but had a very narrow range of activation. Co^{++} produced activation of the enzyme, but was only about 50% as effective as Mg^{++} over the concentration range studied. The optimal metal ion: ATP ratio for Mg^{++},

TABLE V

EFFECTS OF DIVALENT CATION SUBSTITUTION ON NAD^+ KINASE ACTIVITY[a]

Cation	Units	% Activity[b]
Mg^{++}	.505	100
Mn^{++}	.1854	36.7
Ca^{++}	.0942	18.6
Co^{++}	.1283	25.4
Cu^{++}	.0457	9
Ba^{++}	0	0
Fe^{++}	0	0
Zn^{++}	.0367	7.3
Sn^{++}	0	0

[a]See text for Experimental Detail.
[b]Based on 100% activation with Mg^{++}.

Figure 11. Dependence of NAD^+ Kinase Activity on Mg^{++} Concentration.

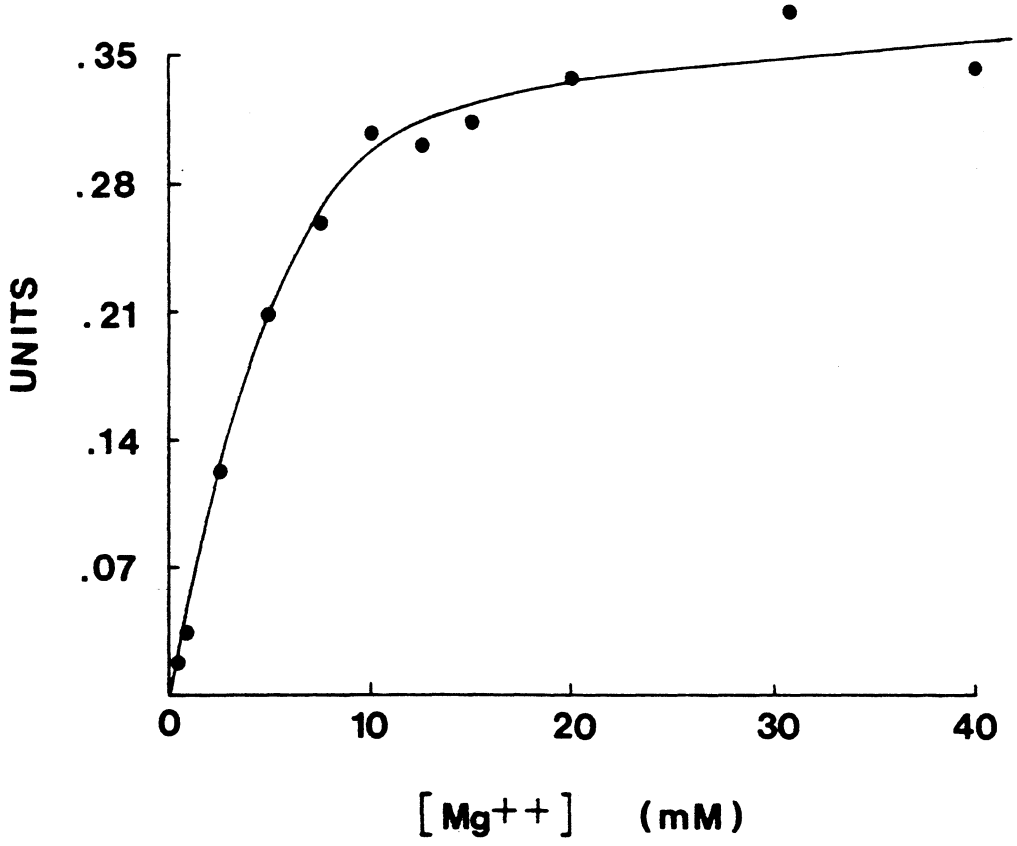
.35
.28
.21
.14
.07
UNITS
0
10
20
30
40
[Mg++] (mM)

Figure 12. Dependence of NAD^+ Kinase Activity on Divalent Cation Concentration.

Divalent cations studied are represented by the following:

Mg^{++} 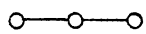

Mn^{++} 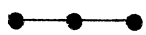

Co^{++} 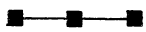

Zn^{++} 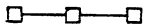

See text for experimental details.

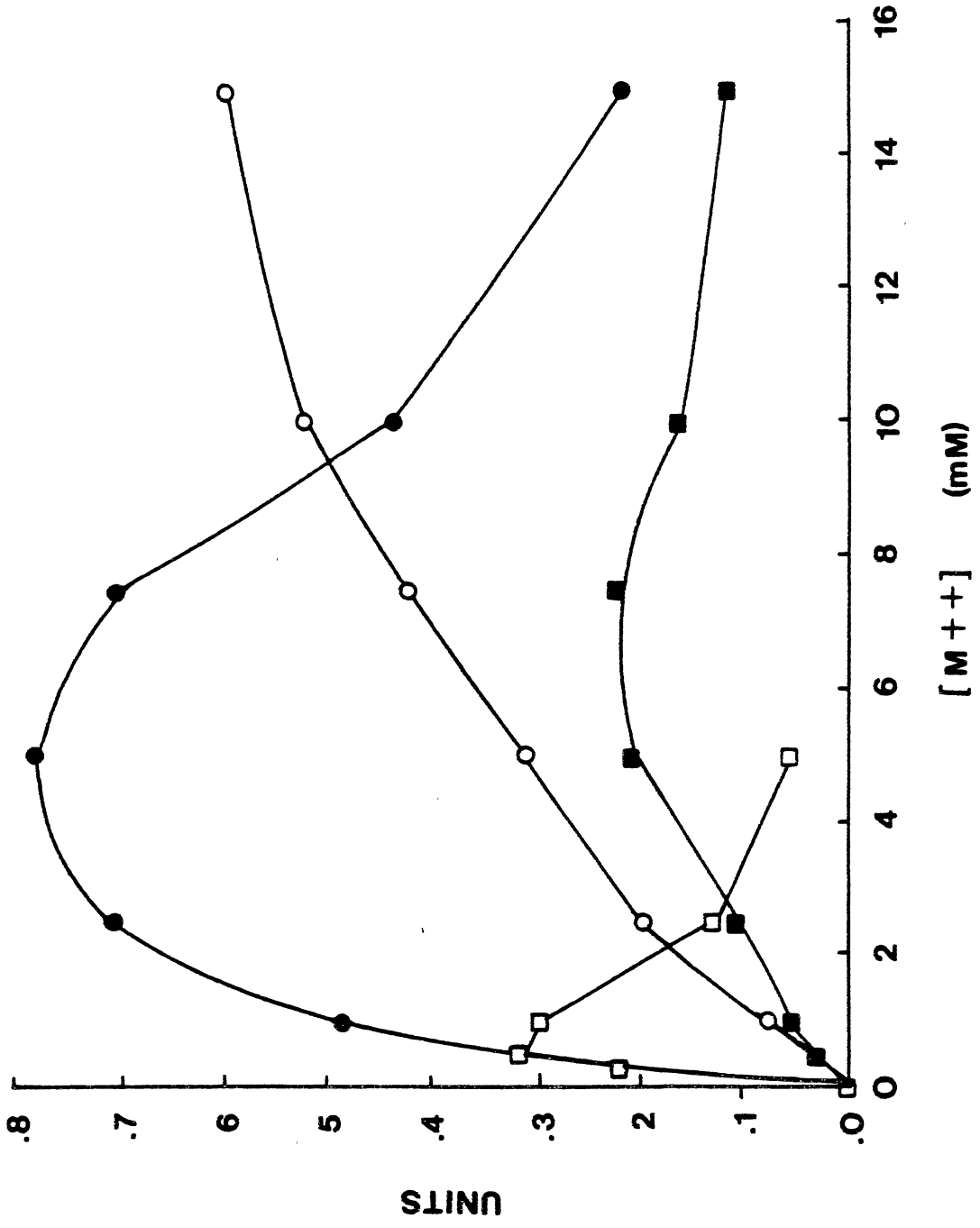
UNITS
.8
.7
.6
.5
.4
.3
.2
.1
.0
0
2
4
6
8
10
12
14
16
[M++] (mM)

Mn^{++}, Co^{++}, and Zn^{++} was 1.5, 0.5, 0.6, and 0.1, respectively. The curves presented in Figure 12 are similar to the findings of Apps (119) for pigeon liver NAD^+ kinase.

pH Optimum

The pH optimum for the NAD^+ kinase assay system was determined by using a series of reaction buffers with a varied pH range from 5.5 to 10. The composition of the buffering system was also varied to determine which buffer gave the highest activity. Reaction mixtures contained 8 mM NAD^+, 10 mM ATP, 15 mM $MgCl_2$, and 0.350 M of the appropriate buffer in a final volume of 0.5 ml. Reactions were initiated by the addition of enzyme and incubated at 37°C. Duplicate reactions were run for 10 and 20 minutes for each buffer and terminated by heating in a boiling water bath for 1 minute. $NADP^+$ produced within the reaction mixtures was determined using the standard spectrophotometric assay. As seen in Figure 13, the NAD^+ kinase assay system has a pH optimum of 7.5. At this pH, MOPS and Tris-HCl were equally effective buffering systems.

Kinetic Analysis of NAD^+ Kinase

For kinetic studies on $NADP^+$ synthesis, NAD^+ kinase was purified through the G-150 step, concentrated by ultrafiltration, and dialyzed for 12 hours against 5 mM l-cysteine, 0.05 M Tris-HCl, pH 8.0 at 4°C. The enzyme was diluted 2-fold with the same buffer and stored at -20°C until used. 150 mM N-ethylmorpholine was used as the reaction buffer. This buffer was chosen due to its non-chelating properties with metal ions (173).

Initial Velocity Studies

The rate of $NADP^+$ production as a function of substrate concentration was studied by varying the NAD^+ concentration at several different fixed concentrations of MgATP. Reaction mixtures contained 150 mM N-ethylmorpholine pH 8.0, 5 mM $MgCl_2$, and

Figure 13. Optimum pH of the NAD^+ Kinase Assay.

The buffering systems used are represented by:

MES ●

MOPS △

Tris-HCl □

Glycine-NaOH ○

See text for experimental detail.

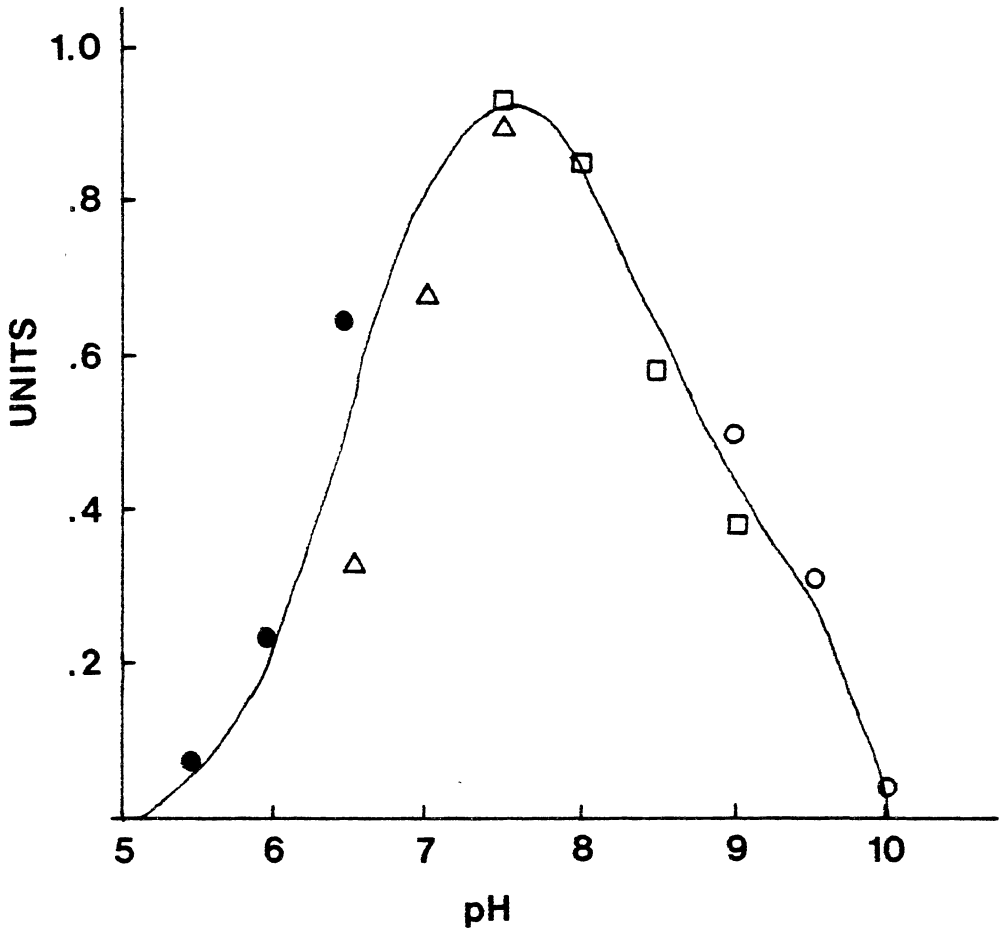
1.0
.8
.6
.4
.2
UNITS
5
6
7
8
9
10
pH

varying concentrations of NAD^+ at fixed levels of MgATP in a final volume of 0.5 ml. The MgATP substrate came from a stock solution of equimolar $MgCl_2$ and ATP which had been adjusted to pH 8.0. At pH 8.0, essentially all the ATP will be complexed with Mg^{++}. In order to insure the free nucleotide species was at negligible concentrations, a 5 mM excess of Mg^{++} was maintained at each concentration of MgATP studied. Reactions were initiated by the addition of enzyme and incubated at 37°C. Duplicate reaction mixtures were assayed for 10 and 20 minutes and terminated by heating in a boiling water bath for 1 minute. $NADP^+$ produced was determined by the standard spectrophotometric assay.

As seen in Figure 14, NAD^+ kinase showed Michaelis-Menton kinetics over an NAD^+ concentration range from 0.5 to 12.5 mM at fixed MgATP concentrations of 2.5 mM, 5.0 mM, 7.5 mM, 10.0 mM, 15.0 mM, and 22.5 mM. An S/v vs S plot for the NAD^+ concentrations used at fixed MgATP levels showed an intersecting pattern of lines (see Figure 15). A similar pattern was observed in Figure 16 for an S/v vs S plot for the MgATP concentrations at various concentrations of NAD^+.

The experimental data used to obtain the curves in Figure 14, was analyzed by the Cleland initial velocity programs described in the Materials and Methods section. A 5% proportional error value was used. The data were fit to the following equations:

1) $Y = VxAxB/ (KIAxKB + KBxA + KAxB + AxB)$

2) $Y = VxAxB/ (KAxB + KBxA + AxB)$

3) $Y = VxAxB/ (KBxA + AxB + KIAxKB)$

A "best fit" was obtained with equation 1 which indicates a sequential mechanism (ordered, Theorell-Chance, or rapid equilibrium). The analysis showed a true Km for NAD^+ of 3.64 mM + 0.42 mM, and a true Km for MgATP of 11.2 mM + 1.32 mM. The calculated V_{max} was 1.1 units.

Figure 14. A Substrate Versus Velocity Plot of NAD^+ Kinase Activity as a Function of NAD^+ and MgATP Concentration.

MgATP concentrations used were:

A 22.5 mM MgATP

B 15.0 mM MgATP

C 10.0 mM MgATP

D 7.5 mM MgATP

E 5.0 mM MgATP

F 2.5 mM MgATP

See text for experimental details.

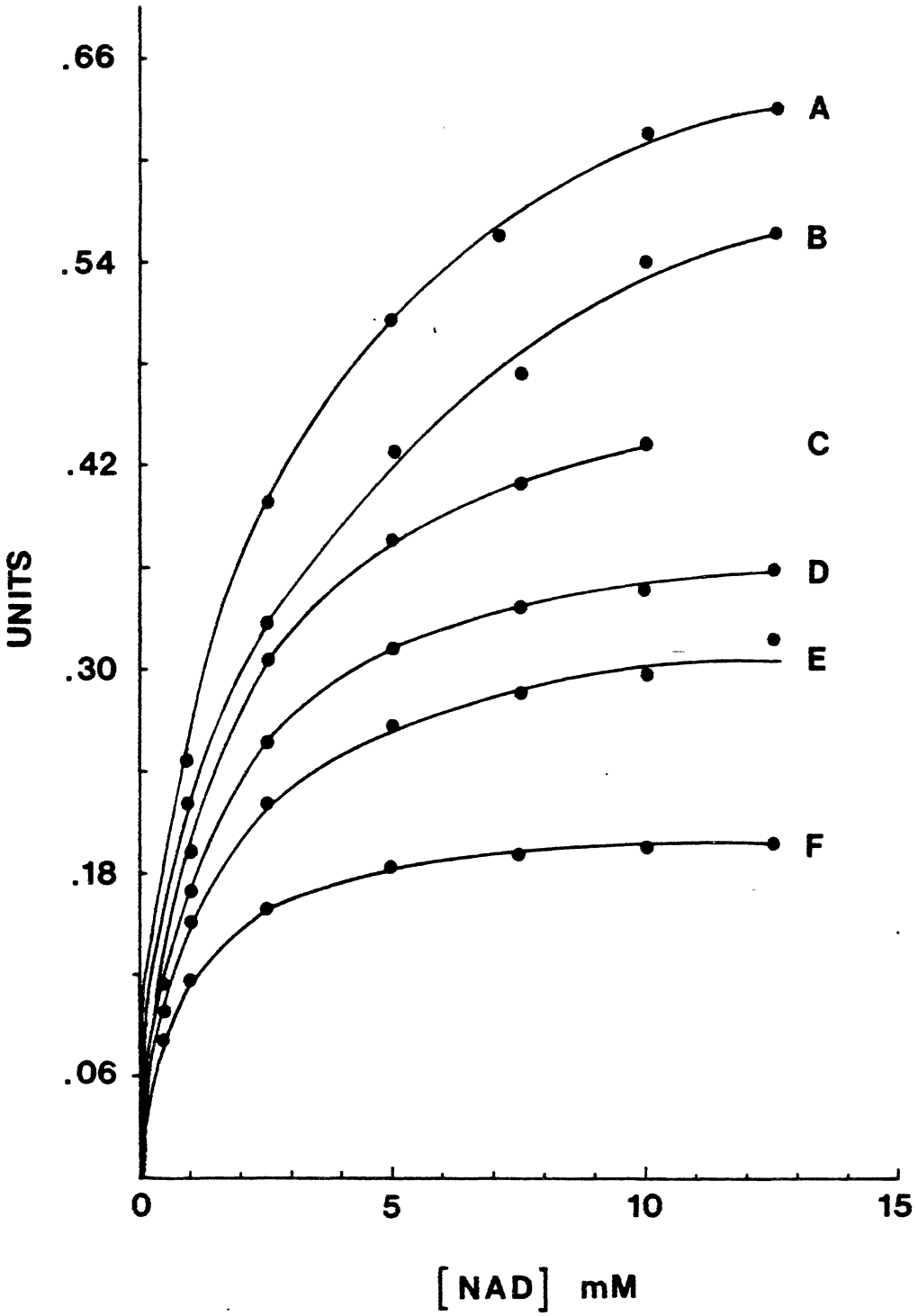
.66
.54
.42
.30
.18
.06
UNITS
A
B
C
D
E
F
0
5
10
15
[NAD] mM

Figure 15. A Substrate/Velocity Versus Substrate Plot of NAD^+ Kinase Activity as a Function of NAD^+ Concentration at Several Fixed Levels of MgATP.

The experimental data from Figure 13 was plotted as an S/V versus S plot with S as NAD^+ at fixed MgATP levels. The fixed levels of MgATP were:

A 2.5 mM MgATP

B 5.0 mM MgATP

C 7.5 mM MgATP

D 10.0 mM MgATP

E 15.0 mM MgATP

F 22.5 mM MgATP

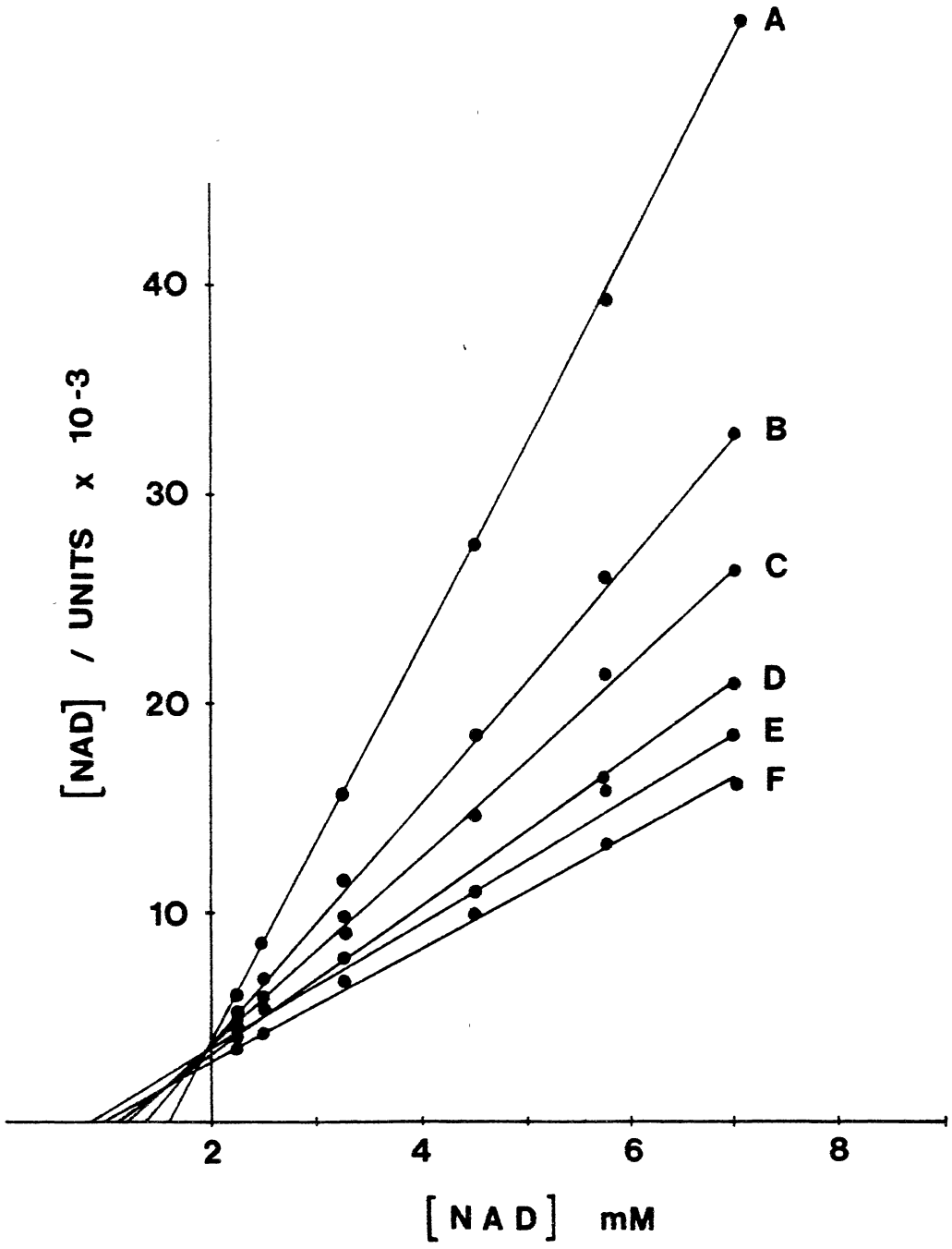
A
B
C
D
E
F
40
30
20
10
[NAD] / UNITS x 10-3
2
4
6
8
[NAD] mM

Figure 16. A Substrate/Velocity Versus Substrate Plot of NAD^+ Kinase Activity as a Function of MgATP Concentration at Several Fixed Levels of NAD^+.

The experimental data from Figure 13 was plotted as as an S/V versus S plot with S as MgATP at fixed NAD^+ concentrations. The fixed levels of NAD^+ were:

A 0.5 mM NAD^+

B 1.0 mM NAD^+

C 2.5 mM NAD^+

D 5.0 mM NAD^+

E 10.0 mM NAD^+

F 12.5 mM NAD^+

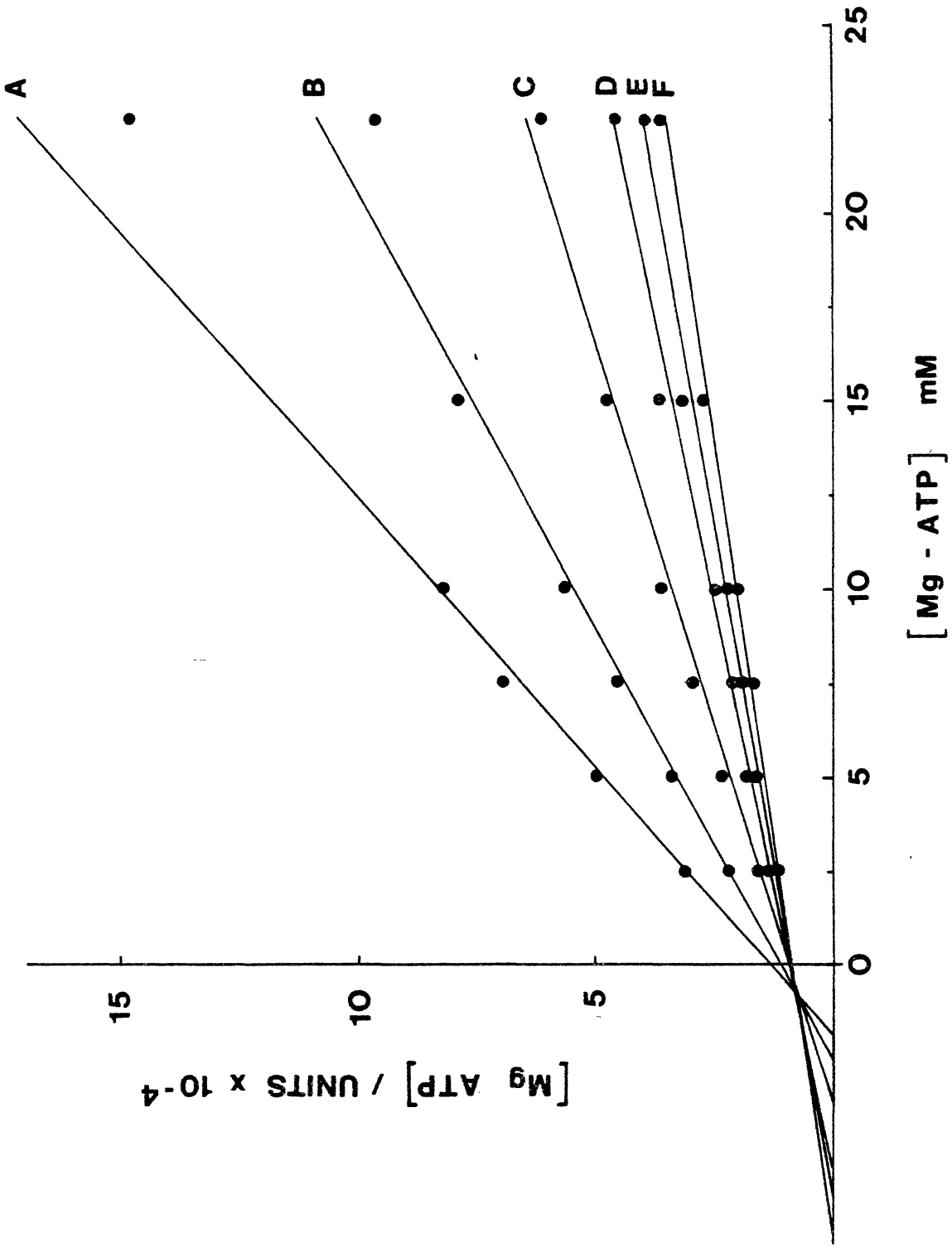
A
B
C
D
E
F
15
10
5
0
5
10
15
20
25
[Mg - ATP] mM
[Mg ATP] / UNITS x 10-4

Product Inhibition Studies

In order to further clarify the mechanism of NAD^+ kinase, product inhibition studies were performed using MgADP. For the first analysis, MgATP was varied at several fixed concentrations of MgADP with the NAD^+ concentration remaining fixed near its Km value. Reaction mixtures contained 150 mM N-ethylmorpholine, pH 8.0, 5 mM $MgCl_2$, 3.5 mM NAD^+ and varying concentrations of MgATP at several fixed concentrations of MgADP. MgATP was used from an equimolar stock solution prepared as previously described. Stock solutions of MgADP were prepared and adjusted to pH 8.0 after calculating the appropriate amounts of Mg^{++} ion to add using the calculations described in the "Materials and Methods" section. Reactions were initiated by the addition of enzyme and incubated at 37°C. Duplicate reaction mixtures were assayed for 10 and 20 minutes and terminated by heating for 1 minute in a boiling water bath. $NADP^+$ synthesized was determined by the standard spectrophotometric assay.

A reciprocal plot of the velocity as a function of MgATP concentration at several different fixed concentrations of MgADP is shown in Figure 17. The observed pattern is indicative of competitive inhibition between MgATP and MgADP.

For the second analysis, NAD^+ was varied at several fixed MgADP levels with the MgATP concentration fixed near its Km at 10 mM. A reciprocal plot of the velocity as a function of NAD^+ concentration at several different levels of MgADP can be seen in Figure 18. The pattern is indicative of noncompetitive inhibition between MgADP and NAD^+.

The experimental data was then analyzed by the Cleland inhibition programs. The proportional error values used for MgADP versus MgATP and MgADP versus NAD^+ were 5% and 7%, respectively. The data were fit to the following equations:

1) $Y = VxA/ (K(1 + I/KI) + A)$

2) $Y = VxA/ (K(1 + I/KIS) + A(1 + I/KII)$

3) $Y = VxA/ (K + A(1 + I/KI)$

Figure 17. A Reciprocal Plot of NAD^+ Kinase Activity as a Function of MgATP Concentration at Several Concentrations of MgADP.

The concentrations of MgADP used are represented by the following symbols:

(□——□) 0.0 mM MgADP

(o——o) 10.0 mM MgADP

(●——●) 25.0 mM MgADP

See text for experimental details.

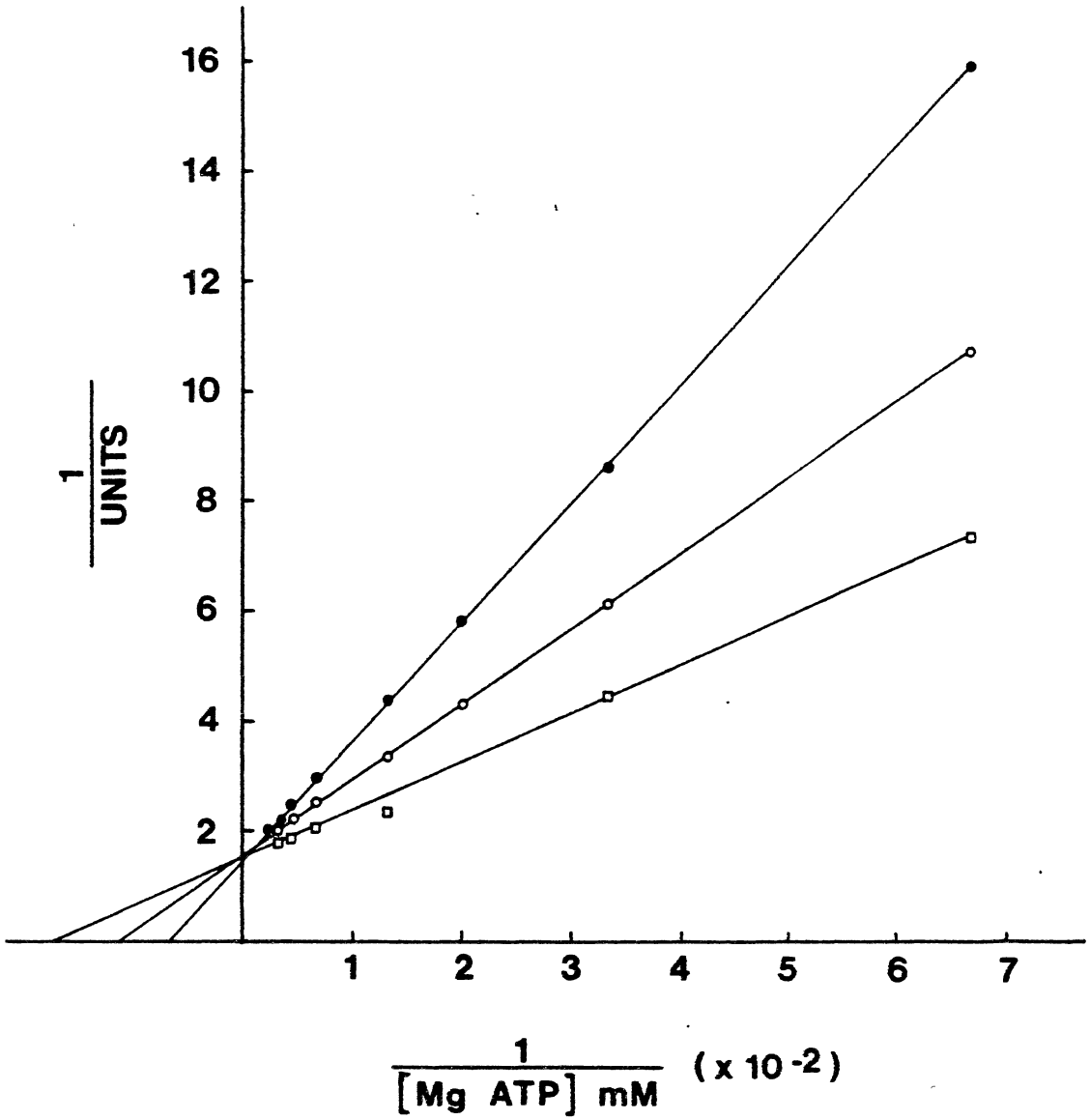
16
14
12
10
8
6
4
2
1
UNITS
1
2
3
4
5
6
7
1
[Mg ATP] mM
(x 10-2)

Figure 18. A Reciprocal Plot of NAD^+ Kinase Activity as a Function of NAD^+ Concentration at Several Fixed Levels of MgADP.

The concentrations of MgADP used are denoted by the following symbols:

(△——△) 0.0 mM MgADP

(□——□) 7.5 mM MgADP

(▲——▲) 15.0 mM MgADP

(■——■) 25.0 mM MgADP

(○——○) 37.5 mM MgADP

(●——●) 50.0 mM MgADP

See text for experimental details.

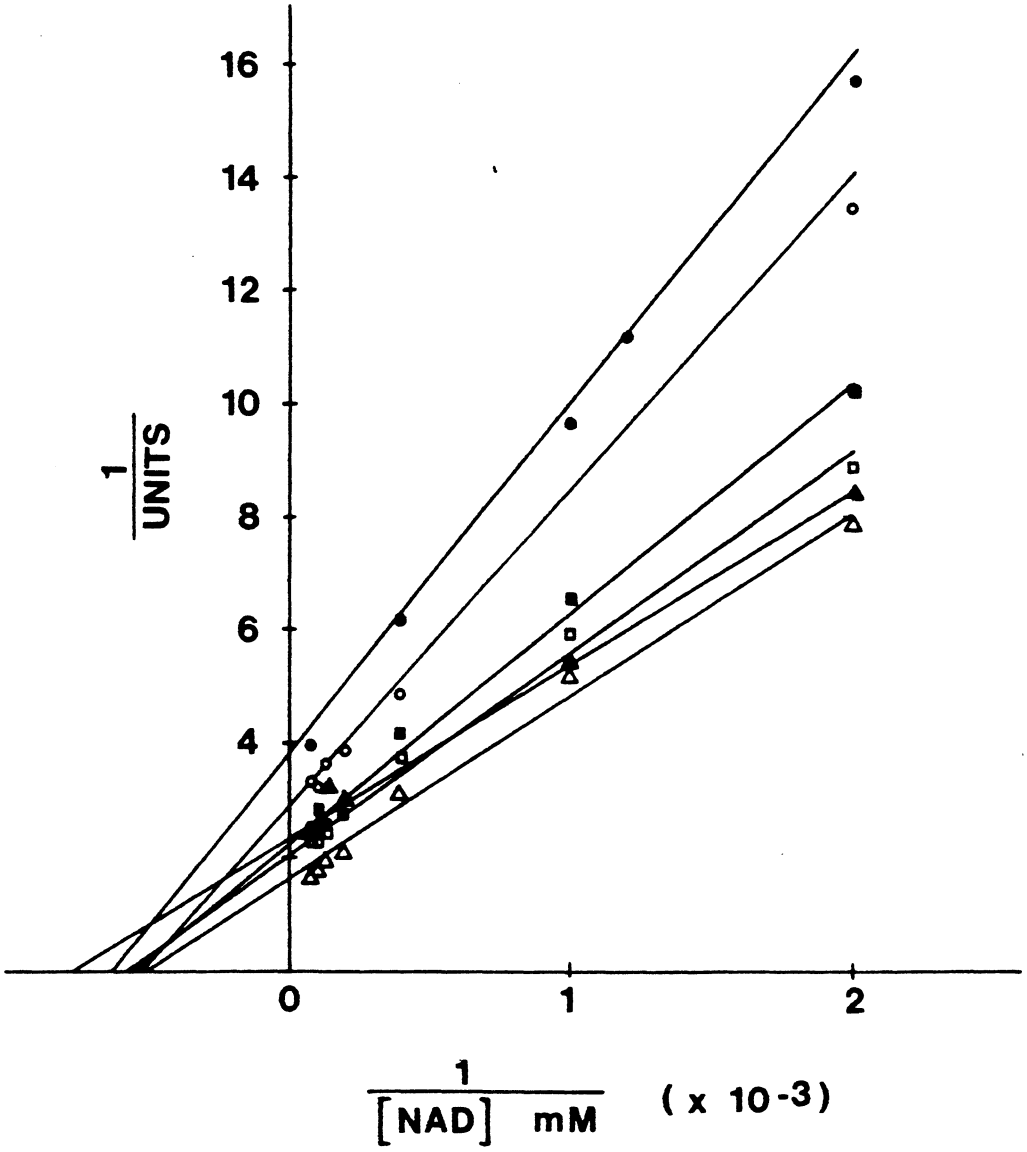
16
14
12
10
8
6
4
1/UNITS
0
1
2
1/[NAD] mM
(x 10-3)

A "best fit" was obtained for MgADP versus MgATP with equation 1 which indicated a competitive-type inhibition. For NAD^+ versus MgADP, a "best fit" was obtained with equation 2 for noncompetitive inhibition. A summary of the kinetic constants and statistical data is presented in Table VI.

Regulation of NAD^+ Kinase

Regulation of NAD^+ Kinase by Ca^{++}/Calmodulin

Within plants, NAD^+ kinase appears to be regulated by Ca^{++}-activated calmodulin. In order to determine if calmodulin plays a role in regulating rat liver NAD^+ kinase, the activity of the enzyme was measured in the presence of increasing concentrations of calmodulin. Reaction mixtures contained 3.5 mM NAD^+, 10 mM MgATP, 50 μM $CaCl_2$, 5 mM $MgCl_2$, 150 mM N-ethylmorpholine, pH 8.0, and varying amounts of calmodulin in a final volume of 0.5 ml. Duplicate reaction mixtures at each level of calmodulin were prepared and initiated by the addition of enzyme. The reaction mixtures were incubated for 10 minutes at 37°C and terminated by heating for 1 minute in a boiling water bath. $NADP^+$ synthesized was determined by the standard spectrophotometric assay. A positive control consisted of calmodulin-deficient 3'-5' cyclic nucleotide phosphodiesterase assayed at the same concentrations of calmodulin. This assay is described in the ' Materials and Methods' section.

As can be seen in Figure 19, NAD^+ kinase activity was not subject to activation by the addition of calmodulin. The positive control, however, was stimulated approximately 6-fold at a calmodulin concentration of 0.137 ng/ml. These results suggested that rat liver NAD^+ kinase was not regulated by calmodulin.

An alternative possibility existed that the enzyme may be already activated by calmodulin and that further increases in calmodulin concentration do not alter the enzyme's activity. This proposal was tested by including trifluoperazine, a potent calmodulin antagonist, in the reaction mixtures. A positive control consisting of the 3'-5' cyclic

TABLE VI

KINETIC CONSTANTS AND STATISTICAL COEFFICIENTS FROM KINETIC STUDIES ON NAD^+ KINASE

Inhibition	Varied Substrate	Type of Inhibition Model	k_{is} (mM)	k_{ii} (mM)	Chi Square/NDF
MgADP	MgATP	Competitive	15.75	—	.7223
MgADP	NAD^+	Noncompetitive	55.37	39.2	1.8176

Figure 19. Effect of Calmodulin on NAD^+ Kinase Activity.

NAD^+ kinase activity is expressed as units and is represented by: ■—■. Cyclic nucleotide phosphodiesterase activity is expressed as nmol. cAMP hydrolyzed per minute and denoted by □—□. See text for experimental details.

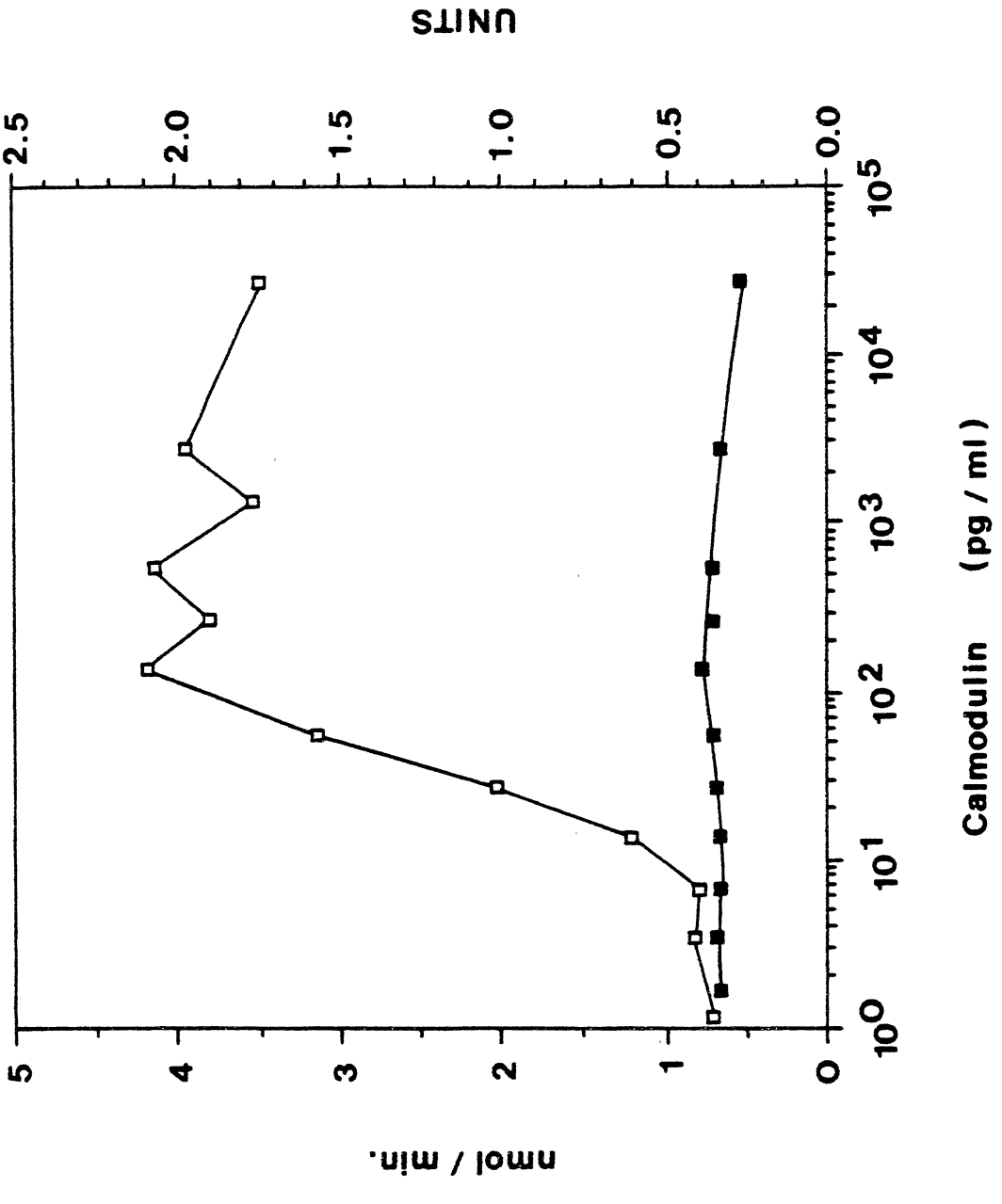
nmol / min.
UNITS
Calmodulin (pg / ml)
0
1
2
3
4
5
0.0
0.5
1.0
1.5
2.0
2.5
10^0
10^1
10^2
10^3
10^4
10^5

nucleotide phosphodiesterase activated with 0.274 ng/ml of calmodulin was used. The results of these experiments can be seen in Figure 20. At 25 μM TFP, an inhibition of 83% is seen in the calmodulin-activated phosphodiesterase control. NAD^+ kinase, however, was not inhibited by TFP over the entire concentration range studied.

Inhibition by Reduced Pyridine Nucleotides

The results of Oka and Field (93) indicate that rat liver NAD^+ kinase may be regulated by reduced pyridine nucleotides. NADH and NADPH appeared to be potent competitive inhibitors of NAD^+ with Ki values of 0.1 mM and 0.05 mM, respectively. The rate of $NADP^+$ formation was inhibited 58% by NADH and 69% by NADPH at inhibitor concentrations of 0.2 mM. $NADP^+$ was a less effective inhibitor at this concentration producing only 6 % inhibition. These results were thus tested with a purer preparation of NAD^+ kinase using similiar substrate concentrations. However, the inhibiting pyridine nucleotides were varied over a wide concentration range from 0.25 to 4.0 mM. In addition, a synthetic analog, 3-acetyl pyridine adenine dinucleotide (APAD) was also tested. Since the presence of NADH, NADPH, and $NADP^+$ would interfere with a spectrophotometric assay, an alternative assay was developed based on the rapid separation of reaction components by HPLC. The HPLC separation method is described under "Materials and Methods". A time course of the assay can be seen in Figure 21.

The results of the inhibition experiments with NADH, NADPH, $NADP^+$, and APAD can be seen in Table VII. At a 0.25 mM concentration, NADH and NADPH inhibited $NADP^+$ synthesis by 67% and 48%, respectively. At the same concentration, $NADP^+$ showed little inhibitory effect. Only at higher concentrations of $NADP^+$ (2.0 to 4.0 mM) did any significant inhibition of NAD^+ kinase occur. APAD appeared to inhibit NAD^+ kinase slightly throughout the concentration range used. These findings support the proposal by Oka and Field (93) that the levels of the reduced pyridine nucleotides influence the rate of $NADP^+$ formation by NAD^+ kinase and may play an important role in regulating

Figure 20. Effect of Trifluoperazine on NAD^+ Kinase Activity.

NAD^+ kinase activity is expressed as units and is denoted by: ●—●. Cylic nucleotide phosphodiesterase activity is expressed as nmol. cAMP hydrolyzed per minute and is represented by: □—□.

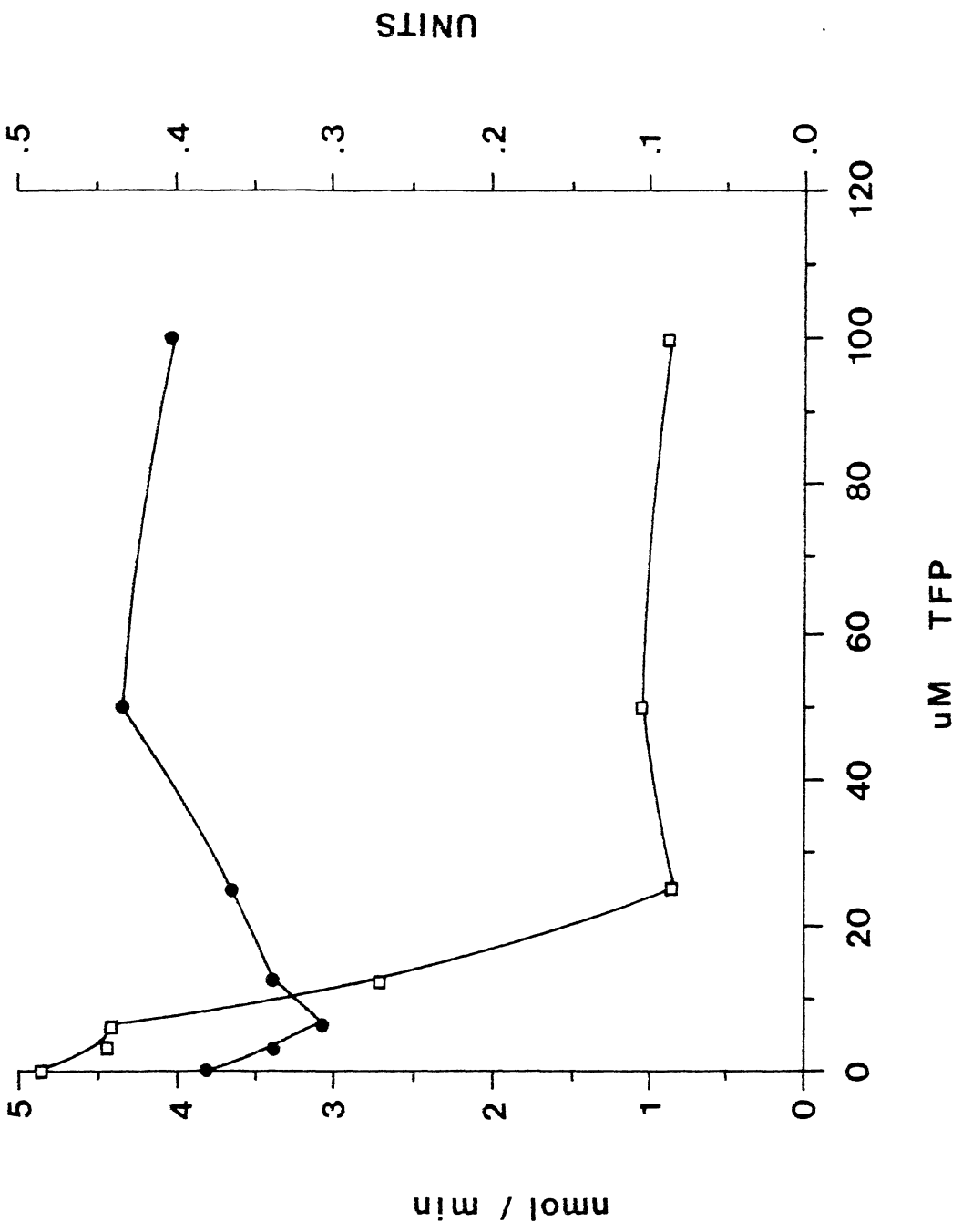
UNITS
.5
.4
.3
.2
.1
.0
120
100
80
60
40
20
0
uM TFP
nmol / min
5
4
3
2
1
0

Figure 21. Time Course of the HPLC-based Assay for NAD^+ Kinase Activity. See text for experimental details.

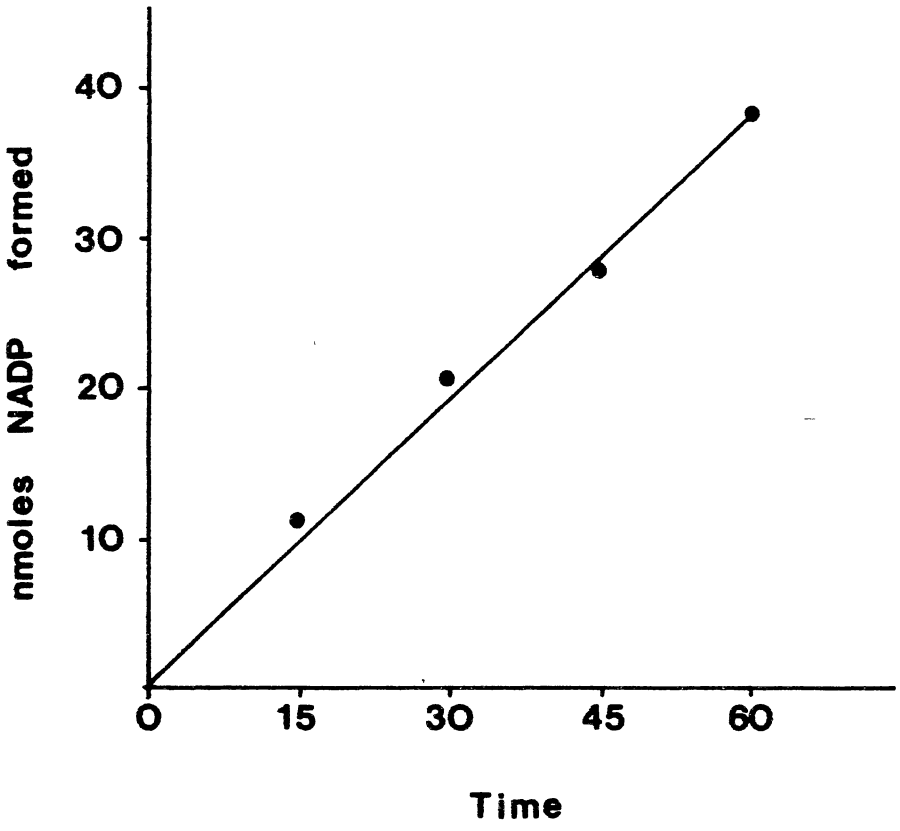
nmoles NADP formed
40
30
20
10
0
15
30
45
60
Time

TABLE VII

EFFECT OF PYRIDINE NUCLEOTIDES ON NAD^+ KINASE ACTIVITY[a]

Inhibitor Concentration	NAD^+ Kinase Activity (Inhibition) with various pyridine nucleotides			
	NADH	NADPH	NADP	HPAD
	Units (%)			
0	0.0636(00.0)	0.0666(00.0)	0.0672(0.0.0)	0.0796(00.0)
0.25 mM	0.0212(66.5)	0.034(48.5)	0.0620(7.5)	0.068(14.5)
0.5 mM	0.0103(83.7)	0.032(48.4)	0.0442(4.5)	0.0752(5.0)
1.0 mM	0.0026(95.9)	0.034(48.5)	0.056(16.7)	0.0685(13.9)
2.0 mM	—	0.0198(70.2)	0.05(25)	0.0643(19.4)
4.0 mM	—	0.0133(80.0)	0.0376(44.5)	0.0652(17.9)

[a]See text for Experimental Details.

the enzyme's activity. One difference, however, was that NADH appeared to be be slightly more effective inhibitor than NADPH in suppressing $NADP^+$ formation.

The development of a reverse-phase HPLC assay for NAD^+ kinase provides a rapid technique for studying the effects of compounds which would otherwise interfere with a spectrophotometric assay. The speed with which the separation of the reaction components is achieved also avoids the somewhat tedious procedures based on traditional Dowex-1 chromatography. The separation of components for the assays used for each inhibiting nucleotide tested routinely took a total time of 4-5 hours.

Modification of NAD^+ Kinase

Several studies on the modification of NAD^+ kinase from various sources have suggested the presence of a sulfhydryl group which is necessary for activity. N-ethylmaleimide (NEM), Ellman's reagent (DTNB), and hydroxymercuribenzoate (HMB) were tested for their ability to inactivate NAD^+ kinase. The sulfhydryl reagents were tested over a concentration range from 0.5 mM to 4.0 mM. Each reagent was pre-incubated with the enzyme and 100 mM N-ethylmorpholine, pH 8.0 for 10 minutes at 23°C. The effects of N-ethylmaleimide were also studied at a lower pH using 200 mM potassium phosphate, pH 7.2. Residual NAD^+ kinase activity was then assayed in reaction mixtures containing 8 mM NAD^+, 10 mM MgATP, 5 mM $MgCl_2$, and 150 mM N-ethylmorpholine, pH 8.0. Duplicate assays were initiated by the addition of 100 µl of the pre-incubation mixtures and incubated for 15 minutes at 37°C. The assays were terminated by heating in a boiling water bath for 1 minute. $NADP^+$ was determined by the standard spectrophotometric assay with the exception that 5 mM l-cysteine was added to the spectrophotometric assay buffer to protect isocitrate dehydrogenase from inactivation by the sulfhydryl reagents.

As can be seen in Figure 22, HMB is a potent inactivator and produces 86% inactivation of NAD^+ kinase at a concentration of 0.2 mM. DTNB was also an effective inactivator of the enzyme at a higher concentrations, producing 93% inactivation at a 4 mM

Figure 22. NAD^+ Kinase Activity as a Function of Sulfhydryl Reagent Concentration.

Sulfhydryl reagents are denoted by the following:

HMB (□——□)

NEM pH 8.0 (■——■)

NEM pH 7.2 (○——○)

DTNB (●——●)

See text for experimental details.

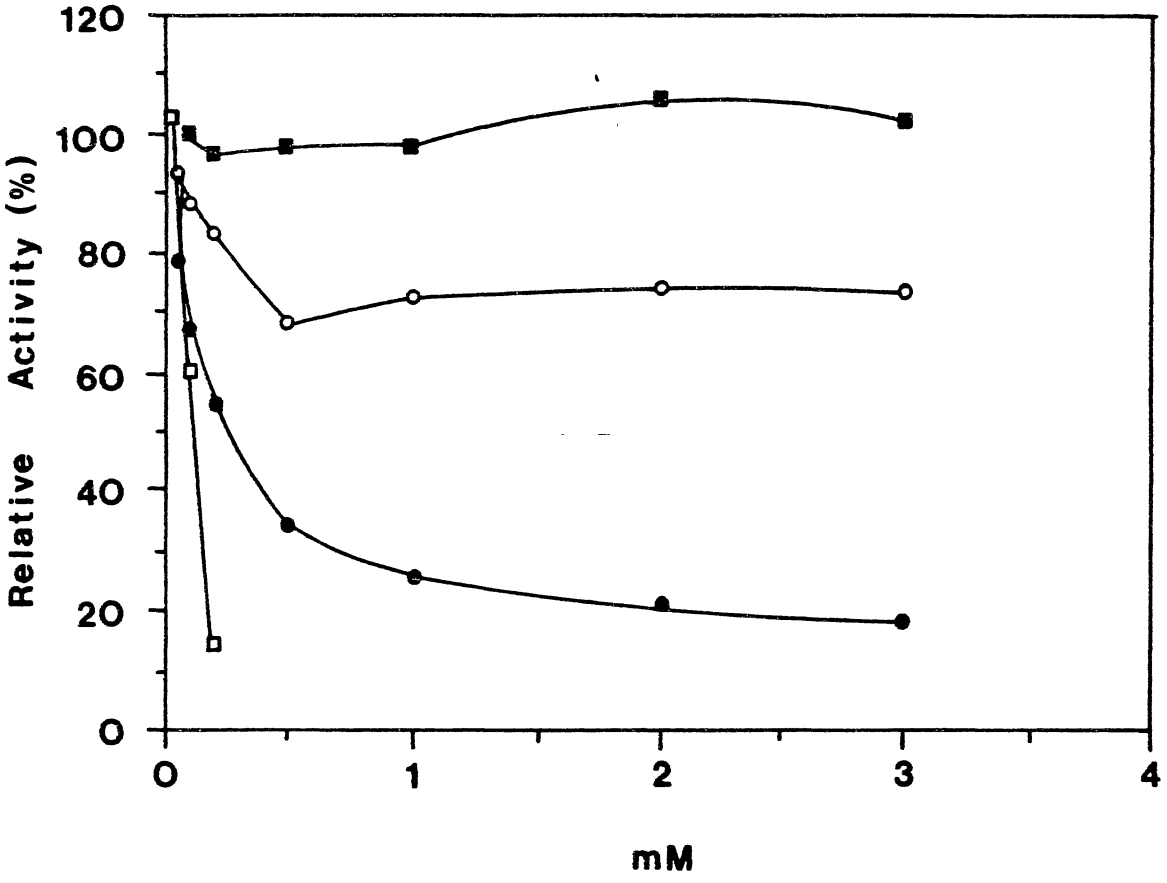
120
100
80
60
40
20
0
Relative Activity (%)
0
1
2
3
4
mM

concentration. N-ethylmalimide, however, produced no inactivation of the enzyme. When N-ethylmaleimide was used at a lower pH, some inactivation of NAD^+ kinase did occur. This result suggested that the sulfhydryl groups of the enzyme may not be reactive toward this reagent or were somehow inaccessible to modification. Based on the differences in inactivation produced by N-ethylmaleimide at different pH's, a more probable explanation is that N-ethylmaleimide was hydrolyzed to N-ethylmaleic acid at the pH's used in the preincubation mixtures. The hydrolysis of N-ethylmaleimide has been reported to occur at pH's above neutral (174).

In order to determine if the inactivation of NAD^+ kinase occurs at an essential sulfhydryl proximal to the active site, the inactivation of NAD^+ kinase was studied in the presence of NAD^+ and MgATP. The results of these experiments are seen in Figure 23. Preincubation of NAD^+ kinase with 8 mM NAD^+, prior to DTNB addition, afforded some protection against inactivation by low concentrations of DTNB. Doubling the concentration of NAD^+ to 16 mM further protected the enzyme from inactivation by DTNB. However, preincubation of the enzyme with 8 mM and 16 mM MgATP did not protect the enzyme from DTNB inactivation. The results suggest that DTNB modifies a sulfhydryl group that may be involved in the binding of NAD^+ by the active site. Further studies on the structure of the enzyme are required to determine if this group is involved in the proper orientation of NAD^+ within the active site or participates directly in catalysis.

The inactivation of sulfhydryl groups by DTNB is reversible. An experiment was performed to determine if DTNB-inactivated NAD^+ kinase can be restored to full activity by the addition of a reducing agent such as dithiothreitol. Table VIII summarizes the results of this experiment. Preincubation of the enzyme with 1 mM DTNB results in 71% inactivation. Addition of 5 mM DTT completely restored the activity of the enzyme.

Figure 23. Substrate Protection of NAD^+ Kinase Activity from Inactivation by DTNB.

Symbols for the graph are as follows:

DTNB (▲——▲)

DTNB + 8 mM NAD^+ (●——●)

DTNB + 16 mM NAD^+ (■——■)

DTNB + 8 mm MgATP (○——○)

DTNB + 16 mM MgATP (△——△)

See text for experimental details.

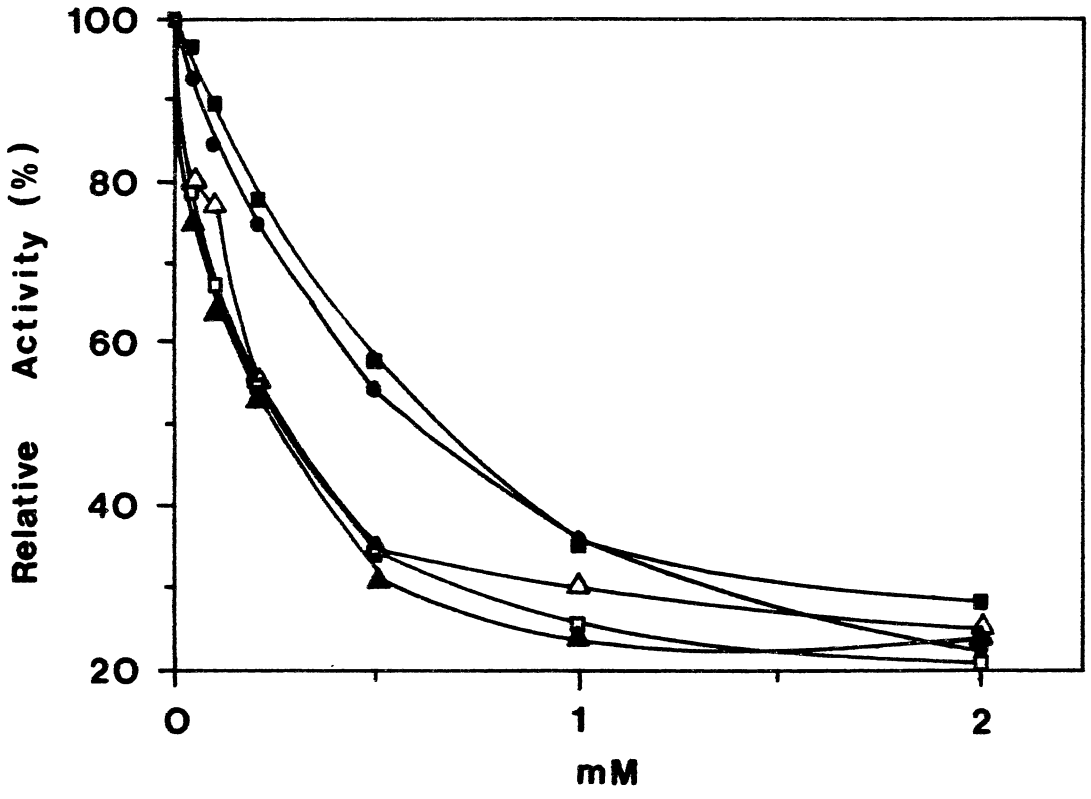
100
80
60
40
20
Relative Activity (%)
0
1
2
mM

TABLE VIII

EFFECT OF DTT ADDITION ON DTNB-INACTIVATED NAD+ KINASE[a]

DTNB Concentration	– DTT	+ DTT
	Units	
0.0	0.5139	0.6297
0.2 mM	0.2820	0.5964
1.0 mM	0.1490	0.6354
2.00 mM	0.096	0.516

[a]See text for Experimental Details.

CHAPTER V

SUMMARY AND CONCLUSIONS

Nicotinamide adenine dinucleotide kinase has been purified over 2000-fold from rat liver. The key steps in the purification scheme are heat treatment, DEAE-Biogel A chromatography, and Blue Sepharose affinity chromatography. Modification of the elution conditions of NAD^+ kinase from the Blue Sepharose column should enhance the purity of the enzyme in the final step of purification. Additionally, exploration of the binding and elution conditions for NAD^+ kinase to other affinity ligands may result in the purification of the enzyme to homgeneity.

Rat liver NAD^+ kinase is rather specific for the nucleoside triphosphates used in the NAD^+ phosphorylating reaction. ATP and dATP were substrates for the enzyme with dATP being a slightly more effective phosphate donor than ATP. NAD^+ kinase, however, is less specific for the divalent cation participating in the reaction. Although MgATP is presumed to be the primary substrate for phosphorylation of NAD^+, cation replacement studies demonstrate that other metal ion-ATP complexes can also serve as substrates for NAD^+ kinase. ATP complexes with Zn^{++}, Mn^{++}, and Co^{++} serve as phosphate donors with the complexes with Zn^{++} and Mn^{++} being more effective than MgATP at lower metal ion concentrations. These findings are in agreement with those of Yero et al. (92) for MnATP and MgATP activation of rat liver NAD^+ kinase and those of Apps (121) for MgATP, MnATP, and ZnATP for pigeon liver NAD^+ kinase. Further studies are required to determine if the alternative metal ion-ATP complexes play a physiologically significant role in regulating NAD^+ kinase activity.

Initial velocity studies on NAD^+ kinase indicate that the enzyme follows a sequential mechanism. Further investigation into the reaction mechanism by product inhibition studies with MgADP yielded the following results: MgADP versus MgATP - competitive inhibition; MgADP versus NAD^+ - noncompetitive inhibition. These data suggest that the reaction mechanism of NAD^+ kinase may follow an ordered pattern of substrate addition and product release. However, further product inhibition studies with $NADP^+$ are required to distinguish between an ordered addition mechanism and a Theorell-Chance or rapid equilibrium random mechanism. Since spectrophotometric assays based on the reduction of $NADP^+$ to NADPH are of limited value in such a study, the development of the HPLC-based assay for NAD^+ kinase should facilitate further investigation into the reaction mechanism of the enzyme.

The NAD^+ kinase isolated from rat liver does not appear to be activated by calmodulin. Addition of Ca^{++} and calmodulin to the enzyme did not result in any stimulation of activity. Secondly, NAD^+ kinase did not have activated calmodulin associated with the enzyme, since the addition of trifluoperazine had little effect on NAD^+ kinase activity. It is of interest to note that calmodulin-dependent NAD^+ kinases seem to be present in systems where there is a primary metabolic event which stimulates a dramatic rise in the levels of $NADP^+$. Such a metabolic "trigger" linked to calmodulin activation of NAD^+ kinase may be absent in cells which are continually requiring $NADP^+$ for oxidation and reduction reactions. However, alternative regulatory mechanisms may exist for controlling the levels of the pyridine nucleotides within complex systems.

Inhibition studies with the reduced pyridine nucleotides show that NADH and NADPH inhibit NAD^+ kinase approximately 67% and 48%, respectively, at a concentration of 0.25 mM. $NADP^+$ did not significantly inhibit the enzyme until higher concentrations (2.0 and 4.0 mM) of the nucleotide were used. These findings support the proposal of Oka and Field (93) that the levels of the reduced pyridine nucleotides may play an important role in the regulation of NAD^+ kinase.

Modification studies with NAD^+ kinase show that the enzyme is susceptible to inactivation by sulfhydryl reagents. HMB totally inactivated the enzyme at concentrations above 0.2 mM. DTNB, which is specific for free sulfhydryls, produces 93% inactivation of the enzyme at a concentration of 4.0 mM. Preincubation of NAD^+ kinase with NAD^+ prior to the addition of DTNB afforded some protection to the enzyme from inactivation by lower concentrations of DTNB. Preincubation of the enzyme with MgATP did not protect the enzyme from DTNB inactivation. This finding suggests that DTNB inactivation of NAD^+ kinase may involve a sulfhydryl group which is proximal to the NAD^+ binding site of the enzyme. Further research is necessary to identify the location of the modified sulfhydryl in the enzyme and its exact function within the enzyme.

The results of this study have answered only a few question concerning the characteristics of NAD^+ kinase from rat liver. It is hoped that these investigations can serve as a background for future research into the mechanism and regulatory properties of NAD^+ kinase and its role in pyridine nucleotide metabolism.

A SELECTED BIBLIOGRAPHY

(1) Harden, A., and Young, W. J. (1904) J. Physiol. 32, Proc.

(2) Von Euler, H., Albers, H., and Schlenk, F. (1936) Z. physiol. chem. 240, 113.

(3) Warburg, O., Christian, W., and Griese, A. (1935) Biochem. Z. 282, 157.

(4) Warburg, O., and Christian, W. (1936) Biochem. Z. 287, 291.

(5) Von Euler, H., and Schlenk, F. (1937) Z. physiol. chem. 246, 64.

(6) Kornberg, A. and Pricer, W. E., Jr. (1950) J. Biol. Chem. 186, 557.

(7) Pullman, M. E., and Colowick, S. P. (1954) J. Biol. Chem. 206, 121.

(8) Pullman, M. E., San Pietro, A., and Colowick, S. P. (1954) J. Biol. Chem. 206, 127.

(9) Loewus, F. A., Venneslandi, B., and Harris, D. L. (1955) J. Am. Chem. Soc. 77, 3391.

(10) Metzler, D. E. (1977) in Biochemistry, The Chemical Reactions of Living Cells, pp. 465-466, Academic Press, New York.

(11) Kaplan, N. O. (1960) in The Enzymes, 3, P. Boyer, H. Lardy, and J. Myrback, eds. pp 105- 169, Academic Press, New York.

(12) Chaykin, S. (1967) Ann. Rev. Biochem. 36, 149

(13) Foster, J. W., and, Moat, A. G. (1980) Microbiol. Rev. 44, 83.

(14) White, H. B., III (1982) in The Pyridine Nucleotide Coenzymes, J. Everse, B. Anderson, and K. S. You, eds. pp. 225-248, Academic Press, New York.

(15) Smith, D.T., Ruffin, J. M., and Smith, S. G. (1937) J. Am. Med. Assn. 109, 205.

(16) Spies, T. D., Cooper, C., and Blankenhorn, M. A. (1938) J. Am. Med. Assn. 110, 622.

(17) Elvenhjem, C. A., Madden, R. J., Strong, F. M., and Wooley, D. W. (1938) J. Biol. Chem. 123, 137.

(18) Preiss, J., and Handler, P. (1957) J. Am. Chem. Soc. 79, 4246.

(19) Priess, J., and Handler, P. (1958) J. Biol. Chem. 233, 488.

(20) Preiss, J., and Handler, P. (1958) J. Biol. Chem. 233, 493.

(21) Imsande, J., and Handler, P. (1958) J. Biol. Chem. 236, 525.

(22) Sundaram, T. K., Rajagopalan, K. V., Pichappa, C. V.. and Sarma, P.S. (1960) Biochem. J. 77, 195.

(23) Imsande, J. (1961) J. Biol. Chem. 236, 1494.

(24) Andreoli, A. J., Ikeda, M., Nishizuka, Y., and Hayashi, O. (1963) Biochem. Biophys. Res. Commun. 12, 92.

(25) Nakamura, S., Ikeda, M., Tsuji, H., Nishizuki, Y., and Hayashi, O. (1963) Biochem. Biophys. Res. Commun. 13 , 285.

(26) Henderson, L. M., Gholson, R. K., and Dalgliesh, C. E. (1963) Comprehensive Bioch. 4, 245.

(27) Dagliesh, C. E. (1955) Adv. Protein Chem. 10, 31.

(28) Krehl, W. A., Teply, L. J., Sarma, P. S., and Elvenhjem, C. A. (1945) Science 101, 489.

(29) Rozen, F., Huff, J. W., and Perlzweig, W. A. (1946) J. Biol. Chem. 163, 343.

(30) Singal, S. A., Briggs, A. P., Sydensticker, V. P., and Littlejohn, J. M. (1946) J. Biol. Chem. 166, 573.

(31) Heidelberger, C., Abraham, E. P., Morgan, A. F., and Lepkovsky, S. (1949) J. Biol. Chem. 179, 143.

(32) Heidelberger, C., Abraham, E. P., and Lepkovsky, S. (1949) J. Biol. Chem. 179, 151.

(33) Henderson, L. M., and Hanks, L.V. (1956) J. Biol. Chem. 222, 1069.

(34) Partridge, C.W.H., Bonner, D. M., and Yanofsky, C. (1952) J. Biol. Chem. 194, 269.

(35) Schayer, R. W., Foster, G. L., and Shemin, D. (1948) Fed. Proc. 8, 248.

(36) Nishizuka, V., and Hayaishi, O. (1963) J. Biol. Chem. 238, 3369.

(37) Davis, D., Henderson, L. M., and Powell, D. (1951) J. Biol. Chem. 189, 543.

(38) Preist, R. E., Bokman, A. H., and Swhweigart, B. S. (1951) Proc. Soc. Expt'l. Biol. Med. 78, 477.

(39) Decker, R. H., Kang, H. H. , Leach, F.R., and Henderson, L. M. (1961) J. Biol. Chem. 236, 3076.

(40) Miyake, A., Bokman, A. H., and Schweigert, B. S. (1954) J. Biol. Chem. 211, 391.

(41) Long, C. L., Hill, H. N., Weinstock, I. M., and Henderson, L. M. (1954) J. Biol. Chem. 211, 405.

(42) Gholson, R. K., Ueda, I., Ogasawara, N., and Henderson, L. M. (1964) J. Biol. Chem. 239, 1208.

(43) Griffith, G.R., Chandler, J. L. R., and Gholson, R. K. (1975) Eur. J. Bioch. 54, 239.

(44) Nasu, S., Wicks, F. D., and Gholson, R. K. (1982) J. Biol. Chem. 257, 626

(45) Wicks, F. D., Sakakibara, S., Gholson, R. K., and Scott, T. A. (1977) Biochim. Biophys. Acta 500, 213.

(46) Nasu, S. and Gholson, R. K. (1981) Biochem. Biophys. Res. Commun. 101, 533.

(47) Nasu, S., Wicks F. D., Sakakibara, S., and Gholson, R. K. (1978) Biochem. Biophys. Res. Commun. 84, 928.

(48) Nasu, S., Wicks, F. D., and Gholson, R. K. (1982) Biochim. Biophys. Acta 704, 240.

(49) Scott, T. A., Bellion, E., Mattey, M. (1969) Eur. J. Biochem. 10, 318.

(50) Scott, T. A., and Mattey, M. (1968) Biochem. J. 107, 606.

(51) Gholson, R. K. (1966) Nature (London) 212, 933.

(52) Kornberg, A., and Lindberg, O. (1948) J. Biol. Chem. 664.

(53) Kornberg, A., and Pricer, W. E., Jr. (1948) J. Biol. Chem. 182, 763.

(54) Handler, P., and Klein, J. R. (1942) J. Biol. Chem. 143, 49.

(55 Jacobson, K. B., and, Kaplan, N. O. (1957) J. Biophys. and Biochem. Cytol. 3, 31.

(56) Yost, D. M., and Anderson, B. M. (1981) J. Biol. Chem. 256, 3647.

(57) Yuan J. H., and Anderson, B. M. (197) J. Biol. Chem. 246, 2111.

(58) Kerns, M., and Natalie, R. (1957) J. Biol. Chem. 231, 41.

(59) Suzuki, N. (1968) J. Vitaminol. 14, 121.

(60) Gopinathan, K. P., Ramakrishnan, T., and Vaidyanathan, C. S. (1966) Arch. Bioch. Biophys. 113, 376.

(61) Gopinathan, K. P., Sirsi, M., and Vaidynathan, C. S. (1964) Biochem. J. 91, 277.

(62) Mather, I. H., and Knight, M. (1972) Biochem. J. 129, 141.

(63) Dietrich, L. S., Fuller, L., Yero, I. L., and Martinez, L. (1965) Nature (London) 208, 347.

(64) Dietrich, L. S., Fuller, L., Yero, I. L., and Martinez, L. (1966) J. Biol. Chem. 241, 188.

(65) Zatman, L. J., Kaplan, N. O., and Colowick, S. P. (1953) J. Biol. Chem. 200, 197.

(66) Walter, P., and Kaplan, N. O. (1963) J. Biol. Chem. 238, 2823.

(67) Kaplan, N. O. (1966) Curr. Aspects Biochem. Energ. 1, 447.

(68) Green, S., Dobrjansky, A., and Bodansky (1969) Cancer Res. 29, 1568.

(69) Astracha, L., Colowick, S. P., and Kaplan, N. O. (1957) Biochim. Biophys. Acta 24, 141.

(70) Vestin, R. (1937) Naturwissenschaften. 25, 67.

(71) Von Euler, H., and Adler, E. (1938) Z. physiol. chem. 252, 41.

(72) Mehler, A. H., Kornberg, A., Grisola, S., and Ochoa, S. (1948) J. Biol. Chem. 174, 961.

(73) Kornberg, A. (1950) J. Biol. Chem. 182, 805.

(74) Katchman, B., Betheil, J. J., Schepartz, A. I., and Sanadi, P. R. (1951) Arch. Biochem. and Biophys. 34, 437.

(75) Wang, T.P., and Kaplan, N.O. (1953) J. Biol. Chem. 206, 311.

(76) Suzuki, K., Nakano, H., and Sakaru, S. (1967) J. Biol. Chem. 242, 3319.

(77) Bernofsky, C. and Utter, M.F. (1968) Science 159, 1362.

(78) Bernofsky C. (1969) FEBS Letters 4, 167.

(79) Griffiths, M.M. and Bernosky, C. (1972) J. Biol. Chem. 247, 1473.

(80) Sanadi, D.R. (1952) Arch. Bioch. Biophys. 35, 268.

(81) Forti, G., Tognoli, C. and Parisi, B. (1952) Biochim. Biophys. Acta 35, 268.

(82) McGuiness, E.T., and Butler, J.R. (1985) Int. J. Biochem. 17, 1.

(83) Middleton, B., and Vignais, P.M. (1961) Biochim. Biophys. Acta 177, 276.

(84) Vignais, P.U. and Vignais, P.M. (1961) Biochim. Biophys. Acta 47, 515.

(85) Field, J. B., Epstein, S. M., Remer, A. K., and Boyles, C. (1966) Biochim. Biophys. Acta 121, 241.

(86) Muto, S., Miyachi, S, Usuda, H., Edwards, G. E., and Bassam, J. A. (1981) Plant, Physiol. 68, 324.

(87) Yamamoto, Y. (1966) Plant Physiol. 41, 523.

(88) Dieter, P., and Marme, D. (1984) J. Biol. Chem. 259, 184.

(89) Butler, J. R., and McGuiness, E. T. (1982) Int. J. Bioch. 14, 839.

(90) Williams, M. B., and Jones, H. P. (1985) Arch. Bioch. Biophys. 238, 81.

(91) Dieter, P., and Marme, D. (1980) Ann. N. Y. Acad. Sci. 356, 371.

(92) Yero, I. L., Farinas, B., and Dietrich, L. S. (1968) J. Biol. Chem. 243, 4885.

(93) Oka, H., and Field, J. B. (1968) J. Biol. Chem. 243, 815.

(94) Nemchiskaya, V. L., Bozkov, U. M., Kushnev, V. P (1970) Biokhimiya 35, 1067.

(95) Fernandes, M. (1970) J. Neurochem. 17, 503.

(96) Severin, S. E., Telepneva, V. I., and Tseitlin , L. A. (1982) (1973) Biokhimiya, 324.

(97) Bulygina, E. E., and Telepneva, V. I. (1980) 45, 2019.

(98) Bulygina, E. E., Busygina, O.G., and Telepneva, V. I. (1982) Biokhimiya 48, 906.

(99) Apps, D. K. (1968) Eur. J. Bioch. 5, 444.

(100) Van Thiet, N., and Telepneva, V. I. (1981) Biokhimiya 46, 435.

(101) Belyaeva, N. F., and Telepneva, V. I. (1973) Dolk. Akad. Nauk. SSSR 209, 977.

(102) Insarov, I. D., Lebedev, A. N., and Telepneva, V. I. (1974) Dokl. Akad. Nauk. SSSR 219, 488.

(103) Blomquist, C. H. (1973) J. Biol. Chem. 248, 7044.

(104) Blomquist, C. H. (1980) Meth. Enzymol. 66, 101.

(105) Anderson, J. M., Charbonneau, H., Jones, H. P., McCann, R. O., and Corimer, M. J. (1980) Biochemistry 19, 3113.

(106) Muto, S., and Miyachi, S. (1977) Plant Physiol. 59, 55.

(107) Apps, D. K. (1970) Eur. J. Bioch. 13, 223.

(108) Tseng, Y. M., Harris, B. G., and Jacobson, M. K. (1979) Biochim. Biophys. Acta 568.

(109) Afanasieva, T.P., Filippovich, S.Y., Sokolovsky, V.Y. and Kritsky, M.S. (1982) Arch. Microbiol. 133, 307.

(110) Chung, A.E. (1971) Meth. Enzymol. XVIII B, 149.

(111) Apps , D. K. (1975) Eur. J. Biochem. 55, 475.

(112) Van Thiet, N.,and Telepneva, V. I. (1981) Bioch. Int. 4, 135.

(113) Gabriel, M. K., and McGuiness, E. T. (1984) FEBS Lett. 175, 419, 421.

(114) Telepneva, V.I. and Insarova, I.D. (1974) Dokl. Akad. Wauk. SSSR 218, 234.

(115) Bulygina, E.R. and Telepneva, V.I. (1982) Biochem. Int. 4, 175.

(116) Dieter, P. and Marme, D. (1980) Ann. N.Y. Acad. Sci. 356, 371.

(117) Walsh, C. (1979) in Enzymatic Reaction Mechanisms, pp. 214-215, W. H. Freeman, San Fransico.

(118) Apps, D. K. (1968) Eur. J. Bioch. 5, 260.

(119) Butler, J. R., and McGuiness, E. T. (1982) Int. J. Bioch. 14, 845.

(120) Apps, D. K., and Marsh, A. (1972) Eur. J. Bioch. 28, 12.

(121) Orringer, B. P., and Chung, A. E. (1971) Biochim. Biophys. Acta 250, 86.

(122) Apps, D. K. (1971) FEBS Lett. 15, 277.

(123) Apps, D. K. (1969) FEBS Letters 5, 96.

(124) Apps, D. K. (1971) Eur. J. Bioch. 19, 301.

(125) Severin, S. E., Telepneva, V. I., and Tseitlin, L. A. (1970) Biokhimiya 36, 1014.

(126) Glock, G. E., and McClean, P., (1955) Biochem. J. 61, 381.

(127) Kaplan, N. O., Goldin, A., Humphreys, S. R., Ciotti, L., and Stolzenbach, F. E. (1955) J. Biol. Chem. 212, 287.

(128) Stollar, V., and Kaplan, N. O. (1961) J. Biol. Chem. 236, 1863.

(129) Dietrich, L. S., and Yero, I. L. (1964) Abstr. 6th int. Congr. Biochem. New York, IX-18, 717.

(130) Clark, J. B., Greenbaum, A. L., and McClean, P. (1966) Biochem. J. 98, 546.

(131) Butcher, F. R., and Serif, G. S. (1967) Biochim. Biophys. Acta 141, 8.

(132) Field, J. B., Epstein, S. M., Remer, A. K., and Boyle, C. (1966) Biochim. Biophys. Acta 121, 241.

(133) Field, J. B., Johnson, P., Kendig, E., and, Pastan, I. (1963) J. Biol. Chem. 238, 1189.

(134) Greenbaum, A. L., Clark, J. B., and McClean, P. (1965) Biochem. J. 95, 167.

(135) Greenbaum, A. L., Clark, J. B., and McClean, P. (1965) Biochem. J. 96, 507.

(136) Goto, K., Laval-Martin, L., and Edmunds, C. M., Jr. (1985) Science 228, 1284.

(137) Epel, D. (1978) in Curr. Top. Devel. Biol., 12, A. A. Moscona and A. Monroy, eds. pp. 186-246, Academic Press, New York.

(138) Steinhardt, R. A., Zucker, R., and Schatten, G. (1977) Devel. Biol. 58, 185.

(139) Krane, S. M., and Crane, R. K. (1960) Biochim. Biophys. Acta 43, 369.

(140) Epel, D. (1964) Biochem. Biophys. Res. Commun. 17, 62.

(141) Epel, D., Patton, C., Wallace, R. W., and Cheung, W. Y. (1981) Cell 23, 543.

(142) Gallien, C. L., Weinman, J., Rainteau, D., Weinman, S. E. (1984) Exp. Cell. Res. 155, 397.

(143) Meijer, L., and Guerrier, P. (1981) Devel. Biol. 88, 318.

(144) Meijer, L., and Guerrier, P. (1982) Biochim. Biophys. Acta 702, 143.

(145) Grisham, M. B., and Everse, J. (1982) in The Pyridine Nucleotide Coenzymes, J. Everse, B. Anderson, and K. S. You, eds. pp. 249 -278,Academic Press, New York.

(146) Beck, W.S. (1958) J. Biol. Chem. 232, 271.

(147) Sparkman, T. B., Johns, T., Engerson, T., and Jones, H. P. (1985) Biochim. Biophys. Acta 846, 8.

(148) Yamamoto, Y. (1962) Plant Physiol. 38, 45.

(149) Oh-Hama, T., and Miyachi, S. (1959) Biochim. Biophys. Acta 34, 202.

(150) Oh-Hama, T., and Miyachi, S. (1960) Plant Cell Physiol. 1, 155.

(151) Ogren, W. L. and, Krogman, D. W. (1965) J. Biol. Chem. 240, 4603.

(152) Muto, S., and Miyachi, S. (1977) Plant Physiol. 59, 55.

(153) Anderson, J. M., and Corimer, M. J. (1978) Biochem. Biophys. Res. Commun. 84, 595.

(154) Anderson, J. M., Charbonneau, H., Jones, H. P., McCann, R. O. , and Corimer, M. J. (1980) Biochemistry 19, 3113.

(155) Nakamura, T., Fujita, K., Eguchi, Y., and Yazawa, M. (1984) J. Biochem 95, 1551.

(156) Marshak, D.R., Clarke, M., Roberts, D. M., and Watterson, D. M.,.

(157) Corimer, M. J., Jarrett, H. W., and Charbonneau, H. C. (1982) in Recent Advances in Ca^{++} and Cell Function, S. Kakiuchi, H. Hidaka, and A. R. Means, eds., pp. 125-139, Plenum Press, New York.

(158) Jarrett,. H. W., DaSilva, T., and Corimer, M. J. (1982) in The Uptake and Utilization of Metals in Plants, D. A. Robb and W. S. Pierpoint, eds.,pp. 205-218, Academic Press, London.

(159) Charbonneau, H. and Corimer, M. J. (1979) Biochem. Biophys. Res. Commun. 90, 1039.

(160) Jarrett, H. W., Charbonneau, H., Anderson, J. M., McCann, R. O., and Corimer, M. J. (1980) Ann. N.Y. Acad. Sci. 356, 119.

(161) Muto, S., Izawa, S., and Miyachi, S. (1982) FEBS Lett 139, 250-254.

(162) Jarrett. H. W., Brown, C. J., Blacks, C.C., and Corimer, M. J. (1982) J. Biol. Chem. 257, 13795.

(163) Wallace, R. W., Tallant, E. A., and Cheung, W. Y. (1983) Meth. Enzymol. 102, 39.

(164) Morrison, J. F., and Cleland, W. W. (1966) J. Biol. Chem. 241, 673.

(165) Gel Filtration, Pharmacia Fine Chemicals, Inc. (1979) Uppsala Sweden.

(166) David, B. S. (1964) Ann. N. Y. Acad. Sci. 121, 404.

(167) Cleland, W. W. (1967) Adv. Enz. 29, 1.

(168) Kennamer, J. E., Sae-lee, J. A., and Gholson, R. K. (1985) Fed. Proc. 44, 4679.

(169) Apps, D. K., and Gleed, D. C. (1976) Biochem. J., 159. 441.

(170) Dean, P. D. G., and Watson, D. H. (1979) J. Chromat. 165, 301.

(171) Qadri, F., and Dean, P.D. G. (1980) Biochem. J. 191, 53.

(172) McGuiness, E. T., and Gabriel, M. K. (1985) Fed. Proc. 44, 3760.

(173) Morrison, J. F. (1979) Meth. Enzmol. 63, 257.

(174) Riordan, J. F., and Vallee, B. L. (1972) Meth. Enzymol. XXV, 449.

VITA

James Edward Kennamer

Candidate for the Degree of

Doctor of Philosophy

Thesis: PURIFICATION AND CHARACTERIZATION OF NAD^+ KINASE FROM RAT LIVER

Major Field: Biochemistry

Biographical:

Personal Data: Born in Twenty-nine Palms, California, June 15, 1959, the son of Mr. and Mrs. Maples J. Kennamer; married to Susan Slater in 1983.

Education: Graduated from McAlester High School in May 1977; received Bachelor of Science degree in Biochemistry form Oklahoma State University in 1981; completed requirements for the Doctor of Philosophy degree at Oklahoma State University in July, 1986.

Professional Experience: Laboratory Technician, Department of Biochemistry, Oklahoma State University May, 1981 to August 1981; Research Assistant, Department of Biochemistry, Oklahoma State University September 1981 to May 1986.